Chapter 19

COMBUSTION CHARACTERISTICS OF HIGHER ALCOHOL/GASOLINE BLENDS

Mridul Gautam and Daniel W. Martin II
Department of Mechanical and Aerospace Engineering
West Virginia University
Morgantown, WV

Abstract

An experimental investigation of combustion characteristics of higher alcohols/gasoline (UTG 96) blends is presented. Lower alcohols (methanol and ethanol) have been used in the past as fuel extenders by mixing them with gasoline, but relatively little work has been reported on higher alcohols (propanol, butanol, and pentanol). All of these alcohols can be produced from coal derived syngas. Given the abundant coal reserves in the United States, use of such higher alcohols offers an attractive alternative to alleviate the country's growing needs for transportation fuels.

Comparisons of knock limits, indicated mean effective pressure (IMEP), emissions, and fuel characteristics between higher alcohol/gasoline blends and neat gasoline were made to determine the advantages and disadvantages of blending alcohol with gasoline. All tests were conducted on a single-cylinder Waukesha Cooperative Fuel Research (CFR) engine operating at steady state conditions and stoichiometric air-to-fuel ratio. The data show that higher alcohol/gasoline blends have a greater resistance to knock than neat gasoline, as indicated by the knock resistance indicator (KRI) and the (RON+MON)/2 antiknock index. Ignition delay and combustion interval data show that higher alcohol/gasoline blends tend to have faster flame speeds.

Other fuel parameters, including reid vapor pressure (RVP) and distillation curve, are affected by the addition of alcohol to gasoline. The lower alcohols (methanol and ethanol) cause the most dramatic increase in RVP and the largest depression of the distillation curve. Addition of higher alcohols (propanol, butanol, and pentanol) tend to curb the effects of methanol and ethanol on RVP and the distillation curves of the blends.

Background

Effect of Alcohol on Antiknock Performance

One of the major attractions of alcohols is their high octane blending value. Each volume percent of an oxygenate added to a typical unleaded gasoline with 87 (R+M)/2 octane rating increases blend octane rating in the range from 0.1 to 0.3 (Unzelman, 1988). In addition, Patel et al. (1987) showed that blends of methanol with higher alcohols increased antiknock performance to a greater degree than methanol alone. However, the Coordinating Research Council, Inc. (1985) and Patel and Henein (1985) have shown that the incremental gains in alcohol/gasoline blend octane rating decrease with increasing alcohol concentration in the blend and increasing octane of the base fuel. Thus, adding

alcohol to premium grade gasoline will not have as dramatic an effect on octane rating as adding alcohol to regular grade gasoline, and the change in octane rating with each volume percent addition of alcohol will become smaller. Further, as with most gasolines, oxygenated blends tend to have less knocking resistance at higher engine speeds. Brinkman et al. (1975) measured the research and motor octane numbers of methanol/gasoline blends using standard ASTM tests, as well as the road octane ratings at various engine speeds using the CRC Modified Borderline technique. Their findings showed that the road octane number, which is the octane rating of a fuel in an on-the-road vehicle, of methanol/gasoline blends decreased with increasing engine speed. However, the research and motor octane numbers, (R+M)/2, increased with increasing methanol in the blend, and the research octane number increased more drastically than the motor octane number with increasing methanol concentration. Their findings also highlighted the decreasing effect of methanol on octane number with increasing methanol concentration.

Alcohol Effects on Distillation, Cold Starting, and Vapor Lock

Adding alcohols to gasoline depresses the boiling temperature of individual hydrocarbons. The lower alcohols cause significant reduction in the front end distillation temperatures, thus affecting primarily the first 50% evaporated. Lower molecular weight alcohols have the greatest effect on boiling point depression. Methanol causes the largest changes; its effects can be observed even when accompanied by a co-solvent. Higher molecular weight alcohols, such as tertiary butyl alcohol (TBA), propanol, butanol, and pentanol, exert smaller changes on the distillation characteristics.

General Motors Research compared the high temperature [26.7^0C - 32.2^0C (80^0F - 90^0F)] driveability and vapor lock performance of methanol blends using six cars with closed-loop fuel control systems: three cars had carburetors, two had throttle body injection, and one car was equipped with multi-port fuel injection (Yaccarino, 1985). Four blends were tested: 3% methanol, 7% methanol, 4.75% methanol with 4.75% TBA, and 8.2% methanol with 2.7% TBA (all percentages are given on volume basis). The blends were matched with two gasolines meeting ASTM specifications for volatility classes C and D, which are fuels designed for typical summer and transitional seasons in the Midwest and Northeastern U.S., respectively. Driveability demerits, which were issued based on hot engine restart, throttle response, and smoothness of engine performance, were greatest for two of the carbureted cars when the alcohol blends were used. The fuel injected cars, and surprisingly one of the carbureted vehicles, performed similarly on the blends and with the gasolines. In the matched volatility vapor lock tests, the carbureted vehicles also performed poorly, with the worst performance from blends containing the highest methanol concentrations. The poor performance of the carbureted cars, even though they had closed-loop control, was to be expected with the alcohol blends. This was due to the fact that carburetors operate at very low pressure differentials and are unable to compensate for volume effects of partially vaporized fuel. Fuel injection systems, on the other hand, can deliver fuel to the injectors at pressure as high as 379 KPa (55 psig) and provide much greater tolerance of volatile fuels than is attainable with carbureted systems.

The property of alcohol fuels that significantly reduces cold starting ability is the heat of vaporization. Alcohols require more heat to vaporize than a typical gasoline.

Bardon et al. (1985) investigated engine response to this factor by measuring the mixture richness required for starting between temperatures of -40^0C and 15.6^0C (-40^0F and 60^0F). The starting performance of a gasoline with an RVP of 61.4 KPa (8.9 psi) was compared to a blend composed of the same gasoline splash-blended with 10% methanol by volume and an RVP of 80 KPa (11.6 psi). The starting performance was not improved with the high RVP blend and, at stoichiometric mixture ratios for each fuel, gasoline allowed the engine to be started at 5^0C (41^0F) whereas the blend would not allow starting below 15^0C (59^0F). A 10% methanol blend matching the 61.4 KPa (8.9 psi) RVP gasoline was also made by removing volatile fractions from the base gasoline. With this blend, the engine would not start at temperatures below 15^0C (59^0F) unless the mixture strength was enriched about 100% above the stoichiometric air-to-fuel of the blend. At -30^0C (-22^0F), gasoline fueled engine could be started only when the mixture was approximately eight times richer than stoichiometric, but the blend with matched RVP required a mixture strength fourteen times richer than stoichiometric. Rich mixtures are always needed to start cold engines, because enough fuel must vaporize to form a combustible air/fuel mixture. Thus, these studies only demonstrate relative difficulties in starting characteristics, not whether an engine will start when fueled with a blend. The relative cold starting difficulties largely depend on the fuel delivery system. The fuel delivery system must be able to provide a rich enough mixture to allow starting with an alcohol/gasoline blend.

EPA Guidelines for Alcohol/Gasoline Blends

The use of alcohols in unleaded gasoline must be approved by the EPA, which must ensure that emission control systems currently in place will not be affected. Thus, there are several EPA guidelines that have to be followed when blending alcohol with gasoline. The "substantially similar" ruling states that alcohol may be added to gasoline provided that the amount of oxygen in the blended fuel does not exceed 2.7% by mass. However, a number of specific proposals have been granted waivers allowing the use of alcohols in gasoline. The ruling followed throughout this research is the "DuPont Waiver." Adopted in January 1985, the DuPont Waiver allows for methanol up to 5.0% volume plus at least 2.5% volume co-solvent (ethanol, propanol, butanol, or pentanol) plus corrosion inhibitor, with maximum oxygen content 3.7% by weight.

Test Engine and Blends

Test Engine

The engine used in this research was the ASTM Cooperative Fuel Research engine manufactured by Waukesha Engine Division, Fuel Research Department, Dresser Industries, Waukesha, WI. The complete unit is known as the "ASTM-CFR Engine*". The Waukesha Engine has been used by several other researchers in their investigation of combustion and emissions characteristics of alcohol fuels and blends (Patel et al., 1987; Hunwartzen, 1982; Harrington and Pilot, 1975; Ebersole and Manning, 1972).

The Waukesha Engine is a four stroke, single-cylinder, spark ignited, and variable compression ratio engine with specifications listed in Table 1. Engine power absorption

* The "ASTM-CFR Engine" is also known as the "Waukesha CFR Engine" or simply the "Waukesha Engine"

and engine motoring capabilities were provided by a 1250 RPM, 3.7 kW (5 HP), 230 V DC dynamometer manufactured by Louis Allis Company, Milwaukee, WI.

Test Blends

Six alcohol/gasoline blends were prepared for this research. As mentioned earlier, these blends followed the EPA DuPont Waiver for alcohol/gasoline blends. Each blend contained 90% (vol) Unleaded Test Gas 96 (UTG 96) from Phillips 66, and 10% (vol) alcohol. The alcohol component of the blends consisted of methanol, ethanol, propanol, butanol, and pentanol (see Table 3.2 for properties of the individual alcohols and UTG 96). While the total concentration was kept constant, the concentrations of individual alcohols in the mix were varied. This was done so that the effect of the individual alcohols, not the total alcohol, could be investigated. In order to decide on the concentrations of the various alcohols in the test blends, extensive tables were made which varied the concentrations of the different alcohols. Table 3 lists the volumetric composition and oxygen content of the six test blends. In addition, the net heat of combustion for each of the six test blends is given in Table 4.

Type	Water cooled-4 cycle
Bore and Stroke	8.26 cm x 11.43 cm (3.250 in x 4.500 in)
Cylinder Swept Volume	611.7 cm^3 (37.331 in^3)
Compression Ratio	4 to 16
Combustion Chamber Volume (at TDC)	176.7 cm^3 to 40.8 cm^3 (10.784 in^3 to 2.489 in^3)
Connecting Rod Length (center-to-center)	25.40 cm (10.000 in)
Piston Rings (number)	5 total (4 compression, 1 oil control)
Ignition System	Spark (coil-points-Champion D16 spark plug)
Weight of Engine (approximate)	399 kg (880 lb)
Weight of Complete Unit (approximate)	1247 kg (2750 lb)

Table 1 - Waukesha Engine Specifications

Property	UTG 96	Methanol	Ethanol	Propanol	Butanol	Pentanol
Chemical Formula	C_8H_{15} (Typical)	CH_3OH	C_2H_5OH	C_3H_7OH	C_4H_9OH	$C_5H_{11}OH$
Molecular Weight	111.21	32.04	46.07	60.10	74.12	88.15
Oxygen Content, wt. %	0.00	49.93	34.73	26.62	21.59	18.15
Stoichiometric A/F	14.51	6.43	8.94	10.28	11.12	11.68
Specific Gravity	0.7430	0.7913	0.7894	0.8037	0.8097	0.8148
Boiling Point, °C (°F)	34-207 (94-405)	65 (149)	78.3 (173)	82.2 (180)	82.7 (181)	–
RVP, KPa (psi)	61.4 (8.9)	32.4 (4.7)	19.3 (2.8)	9.0 (1.3)	18.6 (2.7)	–
Net Ht. of Comb., kJ/L (BTU/gal)	31,913 (114,500)	15,887 (57,000)	21,183 (76,000)	23,970 (86,000)	25,921 (93,000)	26,200 (94,000)
Lat. Ht. of Vaporiz., kJ/L (BTU/gal)	223 (800)	920 (3,300)	725 (2,600)	585 (2,100)	474 (1,700)	251 (900)
RON	96.5	112	111	112	113	–
MON	87.2	91	92	–	–	–

Table 2 - Properties of Pure Alcohols and UTG 96 (Bata et al., 1989; Dorn et al., 1986; Dean, 1992; and Phillips 66, 1995)

	Volume Percentage of						% Volume	% wt. Oxygen
Blend No.	UTG 96	Methanol	Ethanol	Propanol	Butanol	Pentanol	Alcohols	in Blend
1	90.00%	0.60%	2.07%	4.80%	2.40%	0.13%	10.00%	3.03%
2	90.00%	0.60%	0.22%	4.80%	2.40%	1.98%	10.00%	2.72%
3	90.00%	2.00%	2.00%	3.00%	2.88%	0.12%	10.00%	3.34%
4	90.00%	2.00%	2.00%	3.00%	0.12%	2.88%	10.00%	3.24%
5	90.00%	3.24%	2.40%	2.76%	0.13%	1.47%	10.00%	3.70%
6	90.00%	3.04%	2.40%	2.96%	1.47%	0.13%	10.00%	3.70%

Table 3 - Volumetric Composition and Oxygen Content of the Test Blends

Blend ID	kJ/kg	BTU/lb
UTG 96	42912	18448
Blend 1	42751	18379
Blend 2	42744	18376
Blend 3	42779	18391
Blend 4	42798	18399
Blend 5	42828	18412
Blend 6	42821	18409

Table 4 - Net Heat of Combustion of the Six Test Blends and UTG 96

Instrumentation

Overview

Figure 1 illustrates the instrumentation that was installed on the Waukesha Engine to monitor the engine operating parameters and the in-cylinder pressure history. The voltage output from a given sensor was related to the engineering parameter via the calibration information either given by the manufacturer of the particular sensor or generated in the laboratory. Some of the sensors required an “excitation” voltage, so a system of power supplies was constructed to provide the necessary power for the sensors. A 5-volt, a 10-volt, and a 15-volt power supply were used in the power system. Once all the sensors were installed, the voltages output by the sensors were read by an A/D data acquisition board installed in an IBM PC driven by a BASIC 7 program.

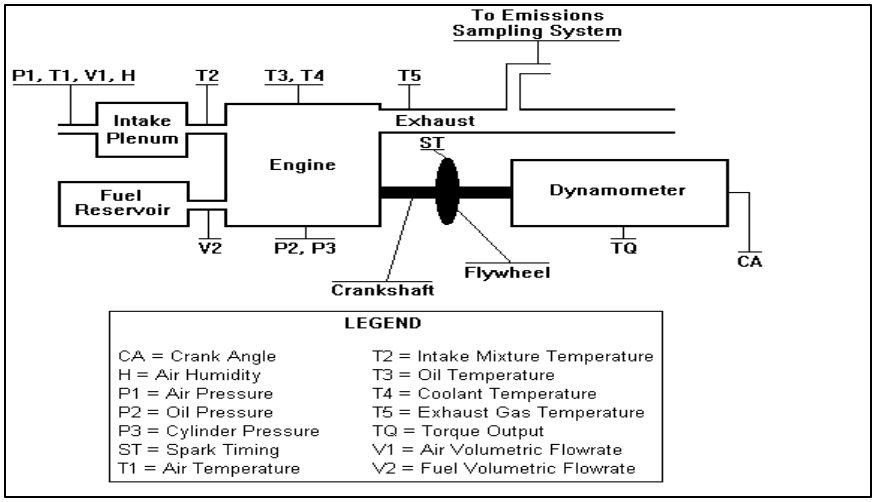

Figure 1 - Schematic of Waukesha Engine Instrumentation

Cylinder Pressure History

In order to evaluate the combustion characteristics (knock intensity, heat release, ignition delay, and burn time) of the alcohol/gasoline blends, a system was developed to capture the in-cylinder pressure history. The system consisted of a piezoelectric pressure transducer, charge amplifier, and power supply was installed on the Waukesha Engine. Piezoelectric pressure transducers contain a piezoelectric crystal, which develops a charge that is proportional to the force acting on the crystal. Then, a charge amplifier converts the induced charge on the crystal into a readable voltage. The high temperatures inside the combustion chamber and in the cylinder head where the pressure transducer was installed, made it imperative to use a water-jacketed transducer. This was necessary for two reasons: (1) piezoelectric pressure transducers experience drift in the output signal with changing temperature and (2) excess heat can destroy a piezoelectric pressure transducer.

Data Acquisition

Overview

With all the necessary transducers in place, a data acquisition system was developed to acquire and archive the test data. An RTI-835L data acquisition board from Analog Devices, which has 16 analog input channels and two digital I/O channels, was used to interface the transducers with a dedicated computer. The board was driven by means of data acquisition software developed in BASIC 7. The board was also capable of timing analog input operations with external events via triggering and pacing. The software used for driving the RTI-835L board employed a BASIC 7 software package from Analog Devices, which is a collection of subroutines that make the board perform its various functions.

Engine Operating Conditions

The voltage signals from various transducers monitoring the engine operating conditions were supplied to the data acquisition board via the analog input channels. One exception was the engine speed. Engine speed was monitored by measuring the frequency of the square wave coming from the crankshaft encoder. The data acquisition board has a counter/timer channel, which is part of the digital I/O section of the board, that can be set up to measure the frequency of an incoming signal. Once the transducers were wired into the data acquisition board, the appropriate subroutines were called from the software package to read the voltages and frequencies coming from the sensors. The calibration information was programmed into the software so that the incoming voltages and frequencies could be converted into corresponding engineering parameters.

The engine operating conditions were monitored and recorded during the blend testing program. All the measured parameters were displayed, in engineering units, on the video monitor.

Cylinder Pressure History

Although the instrumentation for measuring in-cylinder pressures operates in a manner that is similar to the other sensors (that is, converting pressure into a voltage), the initiation of pressure data acquisition had to be indexed with respect to the crank angle. Crank angle resolved in-cylinder pressure measurements (in-cylinder pressure vs. crank angle) were needed for combustion calculations. This was accomplished by a triggered and paced analog input operation. The indexing signal from a cycle position sensor was connected to the external trigger port of the data acquisition board. Thus, the data acquisition operation on the cylinder pressure history was "triggered" by the indexing signal, and the first pressure data point captured would be at the cycle position pre-set by the cycle position sensor. To keep track of the crank angle throughout the rest of the cylinder pressure data acquisition operation, the signal from the crank angle sensor was led into the external pacer port of the data acquisition board. Every fall in the crank angle signal (every half degree of rotation of the crankshaft) would result in an A/D converter command in the data acquisition board. Thus, each pressure data point would be half a degree apart.

The dual use of the crank angle sensor, both as an engine speed sensor and as an external A/D pacer, required the design and construction of an interface. The signal from the crank angle sensor could not be wired into both the frequency measurement port and the external pacer port at the same time due to the limitations of the data acquisition board. Thus, the interface had to be designed so that the signal from the crank angle sensor could be switched between the frequency measurement port and the external pacer port. The interface used signals from the digital output section of the data acquisition board to determine which port the crank angle sensor signal would go to. Thus, the path of the crank angle signal could be controlled from within the data acquisition program. In addition, the interface contained LEDs that indicated when power was available from the 5V, 10V and 15V power supplies, and it also indicated the routing of the crank angle sensor signal via LEDs.

Other Blend Properties

In addition to the combustion and performance characteristics of the blends that were studied on the Waukesha engine tests, the physical and chemical properties of the blends were also studied. These properties include the ASTM D-86 distillation curves, hydrocarbon types, net heat of combustion, Reid vapor pressure, research octane number, and motor octane number. These blend parameters were measured and reported by Core Laboratories, Long Beach, Ca, on a contract basis. Data obtained from Core Laboratories was assured to be in compliance with NIST standards and test procedures.

Data Analysis

Knock Analysis

Knock is an undesirable mode of combustion that originates spontaneously and sporadically in the engine, producing sharp pressure pulses associated with a vibratory movement of the charge and the characteristic sound from which the phenomenon derives its name (Oppenheim, 1988. Knock is associated with an abrupt increase in pressure (large positive curvature) followed by an unusually sharp pressure peak (large negative curvature) and oscillating pressure (many changes in curvature). Since curvature is the second derivative of a signal, a rapid change in curvature would be associated with a large amplitude of the third derivative of the pressure trace. Thus, the maximum amplitude of the third derivative of the pressure trace could be considered as a knock indicator (Checkel and Dale, 1986; Puzinauskas, 1992).

The value of the knock indicator that distinguishes a knocking cycle from a non-knocking cycle will be called the critical knock indicator (CKI). Currently, there is no standard for the value of the CKI; its value is arbitrary and based on experience with the engine and equipment used (Checkel and Dale, 1986). Therefore, several tests were done to determine a reasonable value for the CKI. These tests involved running the Waukesha engine on a stoichiometric mixture of UTG96, at a low compression ratio with no audible knock and spark timing of 15^0 BTDC. Then, the compression ratio was increased in increments of 0.1 until heavy audible knock occurred. At each compression ratio, 50 cylinder pressure traces were captured, and the severity of audible knock was noted. After studying the pressure traces for knock characteristics (sharp pressure rise, sharp pressure peak, and pressure oscillations), analyzing the first and third derivatives of those pressure traces, and comparing the pressure data with audible knock observations, a CKI of 344.7 KPa/degree^3 (50 psi/degree^3) was chosen. The first derivative was calculated numerically using a four-point central difference, Eq. 1, and the third derivative was calculated numerically using a 6-point central difference, Eq. 2 (Chapra and Canale, 1988):

$$f'(x_i) = \frac{-f(x_{i+2}) + 8f(x_{i+1}) - 8f(x_{i-1}) + f(x_{i-2})}{12h} \tag{1}$$

$$f'''(x_i) = \frac{-f(x_{i+3}) + 8f(x_{i+2}) - 13f(x_{i+1}) + 13f(x_{i-1}) - 8f(x_{i-2}) + f(x_{i-3})}{8h^3} \tag{2}$$

Where: h = distance between data points x_i

Figures 2 - 4 illustrate how the knock indicator changes with increasing knock intensity, and how the pressure curve begins to show definite signs of knock around a knock indicator of 344.7 KPa/degree^3 (50 psi/degree^3). In addition, the first derivatives

are also shown to illustrate the spike that occurs with a sharp pressure peak, which is an indication of knock. Further examination of cylinder pressure data taken from the alcohol/gasoline blends also verified that a CKI of 344.7 KPa/degree^3 (50 psi/degree^3) was a valid choice.

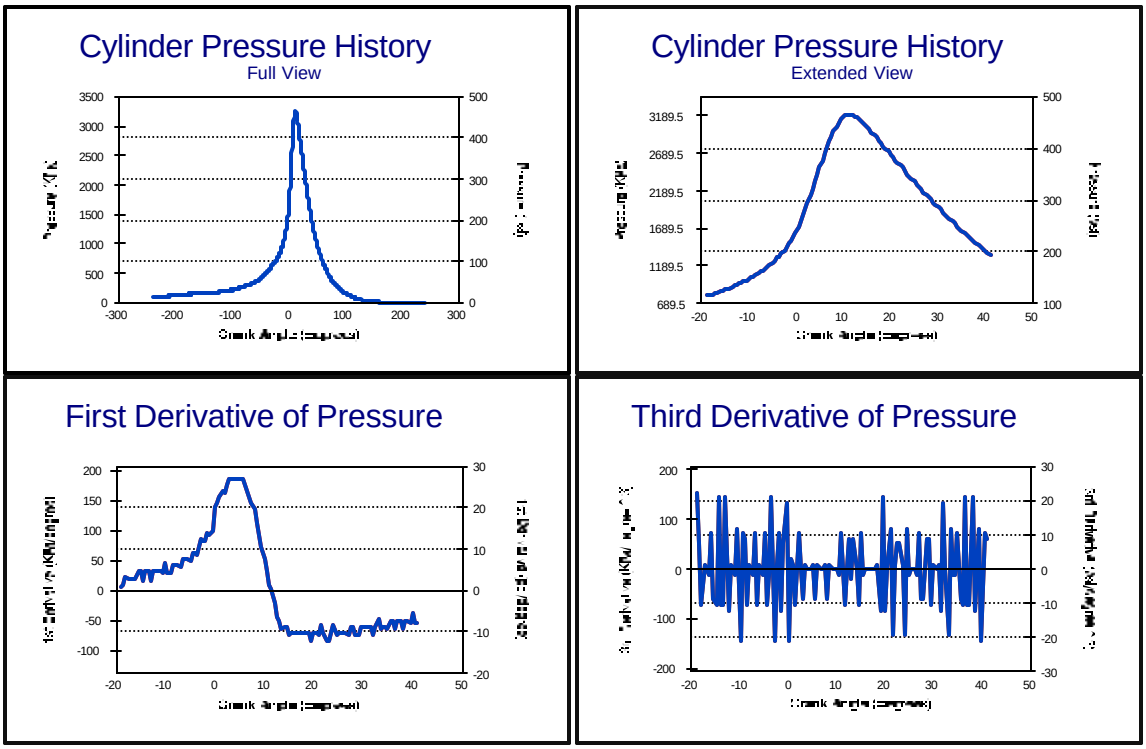

Figure 2 - Pressure trace and derivatives with a knock indicator of 145 KPa/degree^3 (21 psi/degree^3)

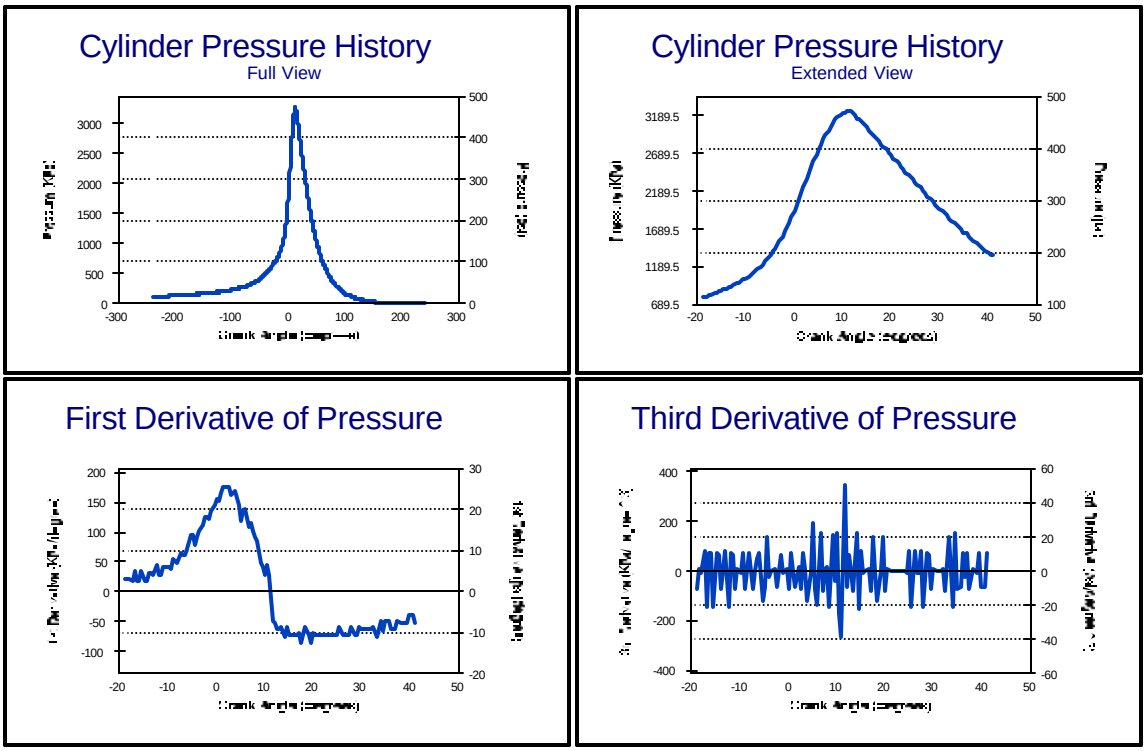

Figure 3 - Pressure trace and derivatives with a knock indicator of 345 KPa/degree^3 (50 psi/degree^3)

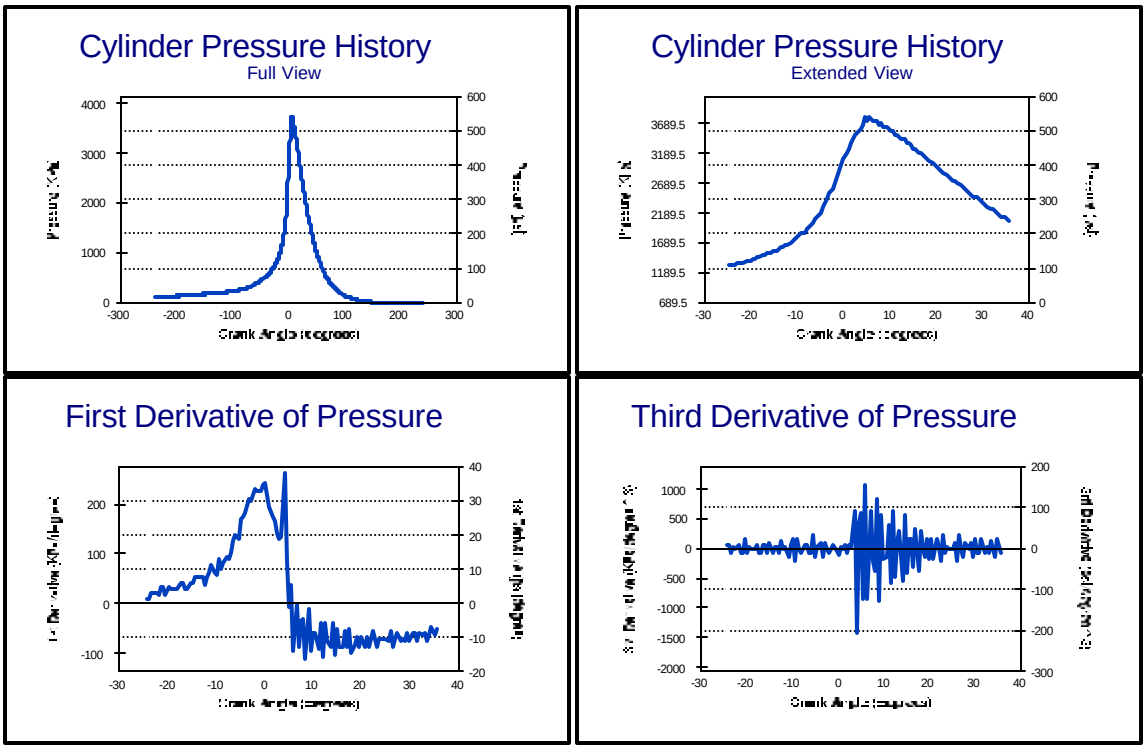

Figure 4 - Pressure trace and derivatives with a knock indicator of 1420 KPa/degree^3 (206 psi/degree^3)

In determining the knock limiting compression ratio (KLCR) for a particular blend at a particular spark timing, 50 pressure traces obtained via the data acquisition procedure were analyzed. The data reduction program calculated the third derivatives of the pressure traces and then kept track of how many of the 50 traces exceeded the CKI. The KLCR was set to the compression ratio (CR) immediately preceding the CR where more than 20% of the pressure curves exceeded the CKI. In other words, the KLCR is the CR corresponding to a particular spark timing where as many as 20% of the cycles are allowed to exceed the CKI, but not more than 20%. The reason for doing this was the cycle to cycle variation. Since the CKI of 344.7 KPa/degree^3 (50 psi/degree^3) identified light knock, there may be a few cycles which showed light knock, but the majority of the cycles were not knocking . Under these conditions, the engine was still running normally.

Indicated Mean Effective Pressure

Indicated mean effective pressure (IMEP) is a measure of the work done by the gas on the piston per unit volume of the cylinder per mechanical cycle. This allows for the comparison of engines of different sizes, because the size of the engine is scaled out. The IMEP can be calculated from a known pressure vs. volume history inside the cylinder. There are two kinds of IMEP: gross IMEP and net IMEP. Net IMEP refers to the work throughout the intake, compression, expansion, and exhaust strokes, while the gross IMEP refers only to the work during the compression and expansion strokes. All further references to IMEP shall designate the gross IMEP.

The IMEP is the net result of the positive work done by the expansion process and the negative work done through the compression stroke. IMEP is calculated by integrating the pressure-volume curve inside the cylinder and dividing by the cylinder swept volume:

$$IMEP = \frac{1}{\pi B^2 S} \int_1^2 P \, dV \tag{3}$$

Where: Point 1 = BDC before the compression stroke
Point 2 = BDC after the expansion stroke
B = cylinder bore
S = piston stroke

Since the crank angle resolved cylinder pressure was measured directly during testing, the integral could be numerically calculated from the experimental data. Using the numerical trapezoidal integration method, Eq. 3 becomes:

$$IMEP = \frac{1}{\pi B^2 S} \sum_{i=\text{BDC before compression}}^{\text{BDC after expansion}} \frac{1}{2}\left(P_{i+1} + P_i\right)\left(V_{i+1} - V_i\right) \tag{4}$$

Volume inside the cylinder can be calculated from crank angle via Eq. 5 (Stone, 1994):

$$V = V_{TDC} + \frac{\pi B^2}{4}\left\{\frac{S}{2}\left(1 - \cos\theta\right) + l - \sqrt{l^2 - \frac{S^2}{4}\sin^2\theta}\right\} \tag{5}$$

Where: V_{TDC} = volume at top dead center
θ = crank angle measured from TDC
l = connecting rod length

Heat Release

The analysis of heat release from the combustion of the air/fuel mixture inside the cylinder of an internal combustion engine provides information on the amount of heat that should be added to the cylinder contents in order to produce the measured pressure variations. With known pressure vs. crank angle data for a particular engine, the rate of heat release from combustion can be calculated from ideal gas principles and thermodynamics. The net rate of heat release can be calculated from the following equation (for a detailed derivation of this equation, refer to Martin II, 1997)

$$\frac{dQ_{HR}^N}{d\theta} = \frac{V_\theta}{(\gamma - 1)\ \Delta\theta}\left(P_\theta - P_{\theta-\Delta\theta}\left[\frac{V_{\theta-\Delta\theta}}{V_\theta}\right]^\gamma\right) \tag{6}$$

Where: $\frac{dQ_{HR}^N}{d\theta}$ = the net heat release rate $\left(\text{BTU}/\text{degree}\right)$
P_θ = measured pressure at crank angle θ
V_θ = cylinder volume at crank angle θ

$P_{q-\Delta q}$ = measured pressure at crank angle $(\theta - \Delta\theta)$

$V_{q-\Delta q}$ = cylinder volume at crank angle $(\theta - \Delta\theta)$

γ = ratio of specific heats ≈ 1.3

In order to identify the portion of the heat release curve that signifies the combustion event, a search algorithm was used to find the maximum heat release rate. The *beginning* of combustion was then set to the crank angle corresponding to the first negative or zero value for heat release *preceding* the maximum heat release. Similarly, the *end* of combustion was set to the crank angle corresponding to the first negative or zero value for heat release *following* the maximum heat release. In an effort to eliminate the effects of cycle to cycle variations, the 50 pressure curves obtained at each setpoint were averaged together to obtain an average pressure history. Heat release analysis was then performed on the average pressure curve.

Mass Fraction Burned, Ignition Delay, and Combustion Interval

Mass fraction burned (MFB) profiles for a combustion process in an internal combustion engine can be derived from the heat release data. Assuming that the amount of heat added is directly proportional to the amount of fuel burned, the MFB can be calculated by integrating the heat release curve up to the point of interest and dividing by the total heat released:

$$\mathrm{MFB} = \frac{\sum_{i=BC}^{P} \left(\frac{dQ_{HR}^{N}}{d\theta} \right)_i}{\sum_{i=BC}^{EC} \left(\frac{dQ_{HR}^{N}}{d\theta} \right)_i} \tag{7}$$

Where: *BC* is the beginning of combustion
EC is the end of combustion
P is the point of interest in the combustion event

Values for MFB will range from 0% to 100%..

Ignition delay, $\Delta\theta_{ID}$, is defined as the crank angle interval between the spark discharge and the time when a small but significant fraction of the cylinder mass has been burned or fuel chemical energy has been released. $\Delta\theta_{ID}$ is usually taken to be the difference between crank angles corresponding to spark discharge and 10% MFB. In addition, the combustion interval, $\Delta\theta_{CI}$, is defined as the crank angle interval required to burn the bulk of the charge and is usually taken as the difference between crank angles corresponding to 10% MFB and 90% MFB (Heywood, 1988).

Results and Discussion

Overview

Since the objective of this study was to evaluate the combustion characteristics of higher alcohol/gasoline blends and compare those characteristics to neat gasoline the engine was operated at steady state with certain engine operating conditions held constant. This permitted the measurement and analysis of combustion characteristics as a function of the fuel used in the engine and not the engine itself. Table 5 lists the engine operating conditions used in this study:

Engine Parameter	Specification
Speed	895 - 905 RPM
Intake Manifold Temperature	45^0C - 47.2^0C (113^0F - 117^0F)
Crankcase Oil Temperature	64.4^0C - 67.8^0C (148^0F - 154^0F)
Coolant Water Temperature	97.2^0C - 98.3^0C (207^0F - 209^0F)
Air / Fuel Ratio	Stoichiometric

Table 5 - Engine Operating Conditions During Blend Testing

The main combustion characteristic of interest with the alcohol/gasoline blends was the knock limiting compression ratio (KLCR), which is defined here as the maximum compression ratio at a given ignition timing where the engine will operate without excessive knock. To determine whether or not the engine was knocking excessively, the pressure history inside the cylinder was used. Since the KLCR is a function of ignition timing, the testing procedure consisted of capturing cylinder pressure traces at various ignition timings and compression ratios. Ignition timing was varied between 30^0 BTDC and 0^0 in increments of 2.5^0. At each ignition timing, acquisition of cylinder pressure histories began at a compression ratio (CR) well below the KLCR (audible knock) Then, the CR was increased in increments of 0.1 until excessive audible knock occurred, and cylinder pressure histories were captured at each ignition timing-compression ratio setpoint. To ensure that cycle-to-cycle variation did not influence the analysis of knock, 50 pressure traces were captured at each ignition timing-compression ratio setpoint.

Once the KLCR for each ignition timing was determined, the ignition timing-KLCR combination that produced the best IMEP was identified. Similar to knock analysis, IMEP was also determined from the cylinder pressure histories. Once the best IMEP point was identified, the other combustion parameters (heat release, burn time, and ignition delay) were also compared at the point of best IMEP. It should be noted that the point of best IMEP is also the point of maximum engine power. Thus, the engine performance parameters were being compared when the engine spark timing and compression ratio were optimized for a particular blend.

Knock Limits and IMEP Trends

The knock limit curves and IMEP trends were plotted versus spark timing for each blend and UTG 96 in Figures 5 - 11. The IMEP data were generated at the corresponding spark timing/KLCR combinations. Figures 5 - 11 show, as expected, that the KLCR increased with increasingly retarded spark timing. In addition, the IMEP also increased with the spark timing/KLCR combinations from 30^0 BTDC up to about 17.5^0 BTDC, leveled off, and then continued to increase up to 5^0 BTDC. Thus, the point of maximum engine power for each blend and UTG 96 was at spark timing 5^0 BTDC and the corresponding KLCR. Table 6 summarizes the spark timing/KLCR combinations where the best IMEP was obtained for each blend. It should be noted that every blend produced a better IMEP than UTG 96. This was undoubtedly due to the better anti-knock characteristics of the blends which allowed higher compression ratios.

Blend ID	Spark Timing @Best IMEP	Compression Ratio @ Best IMEP	Best IMEP KPa (psi)
UTG 96	-5.0	8.8	275.9 (40.01)
1	-5.0	9.5	337.1 (48.89)
2	-5.0	9.4	338.1 (49.04)
3	-5.0	9.9	355.1 (51.50)
4	-5.0	9.4	338.7 (49.13)
5	-5.0	9.9	358.7 (52.02)
6	-5.0	9.9	356.9 (51.76)

Table 6 - Engine Settings for Best IMEP for Each Blend and UTG 96

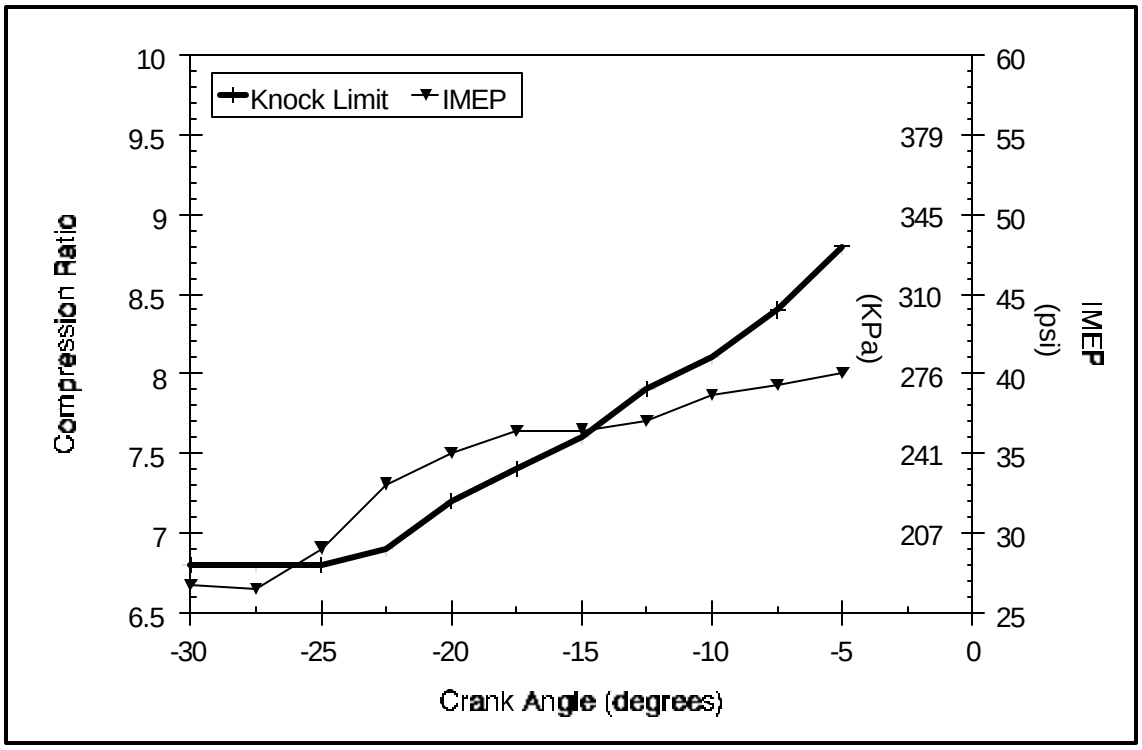

Figure 5 - Knock Limits and IMEP Trend for UTG 96

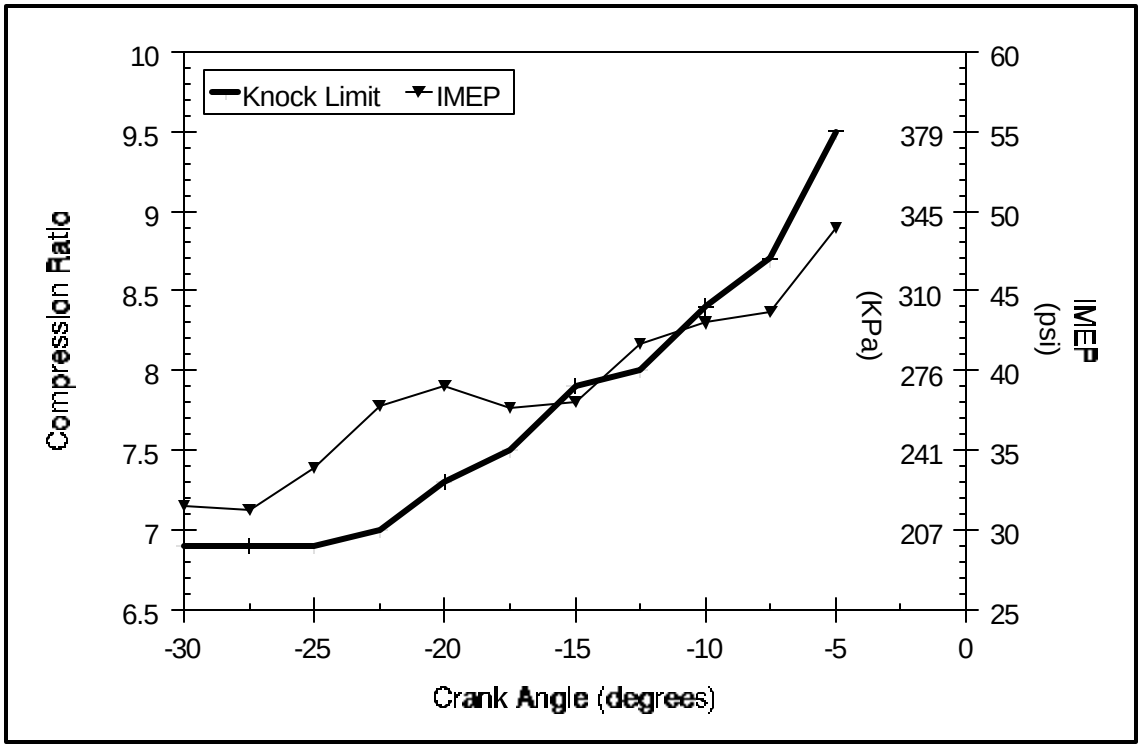

Figure 6 - Knock Limits and IMEP Trend for Blend 1

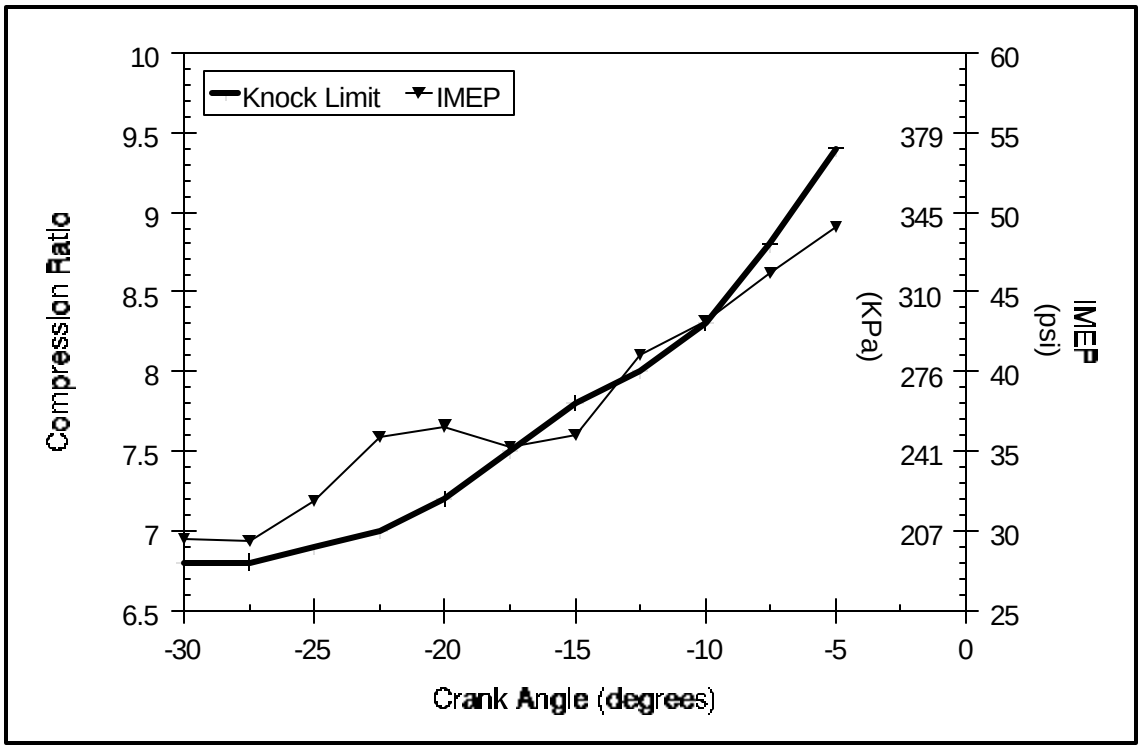

Figure 7 - Knock Limits and IMEP Trend for Blend 2

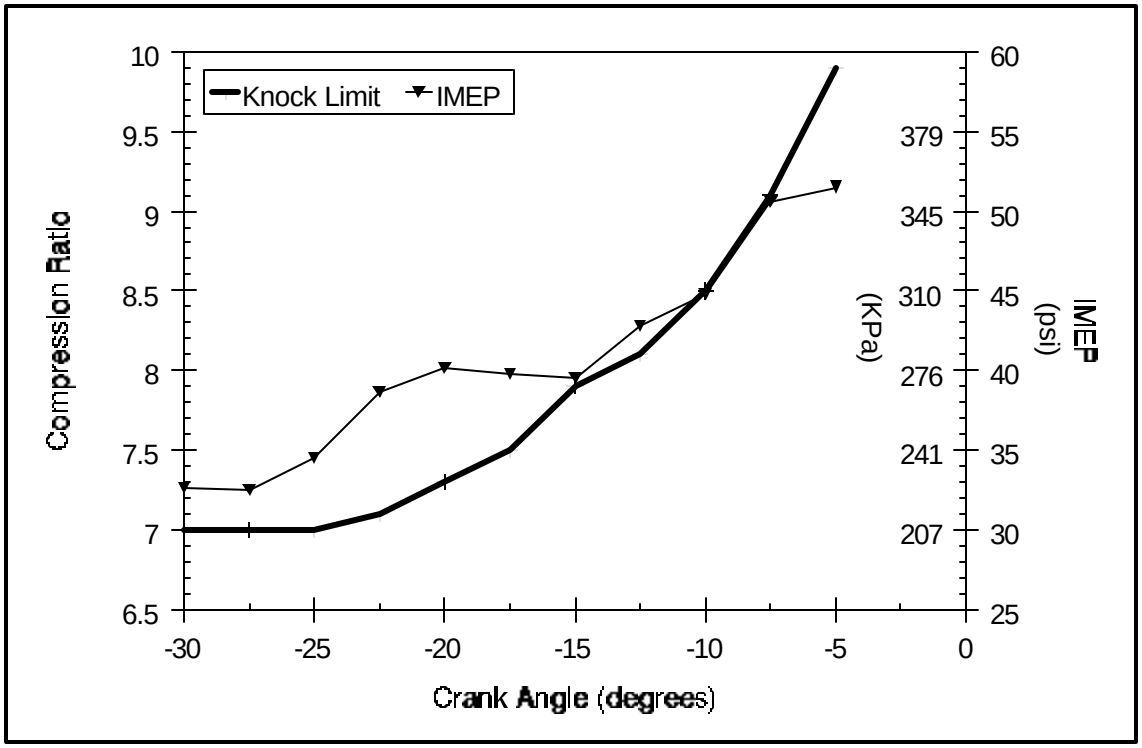

Figure 8 - Knock Limits and IMEP Trend for Blend 3

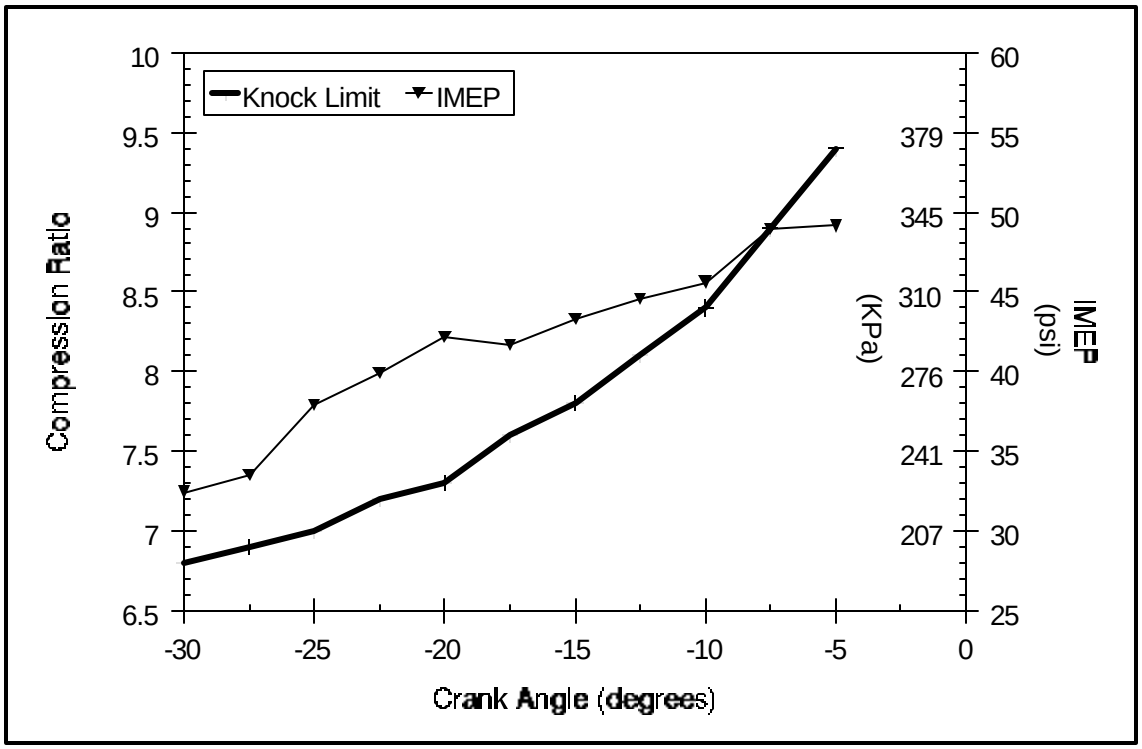

Figure 9 - Knock Limits and IMEP Trend for Blend 4

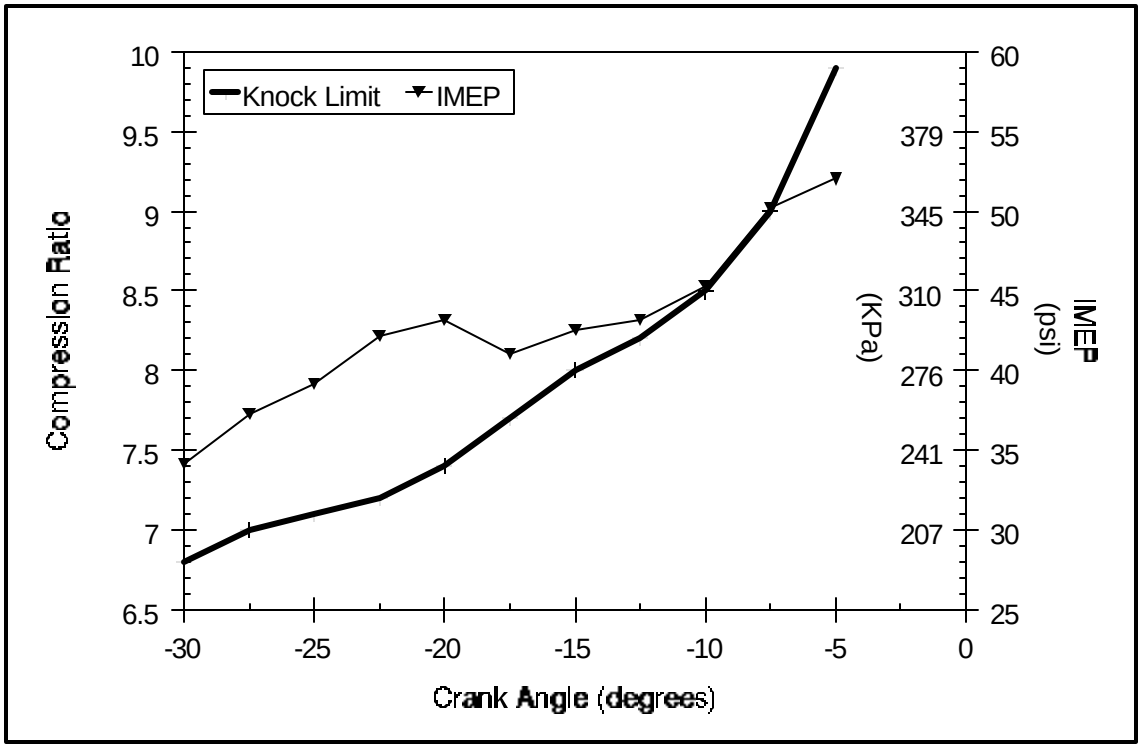

Figure 10 - Knock Limits and IMEP Trend for Blend 5

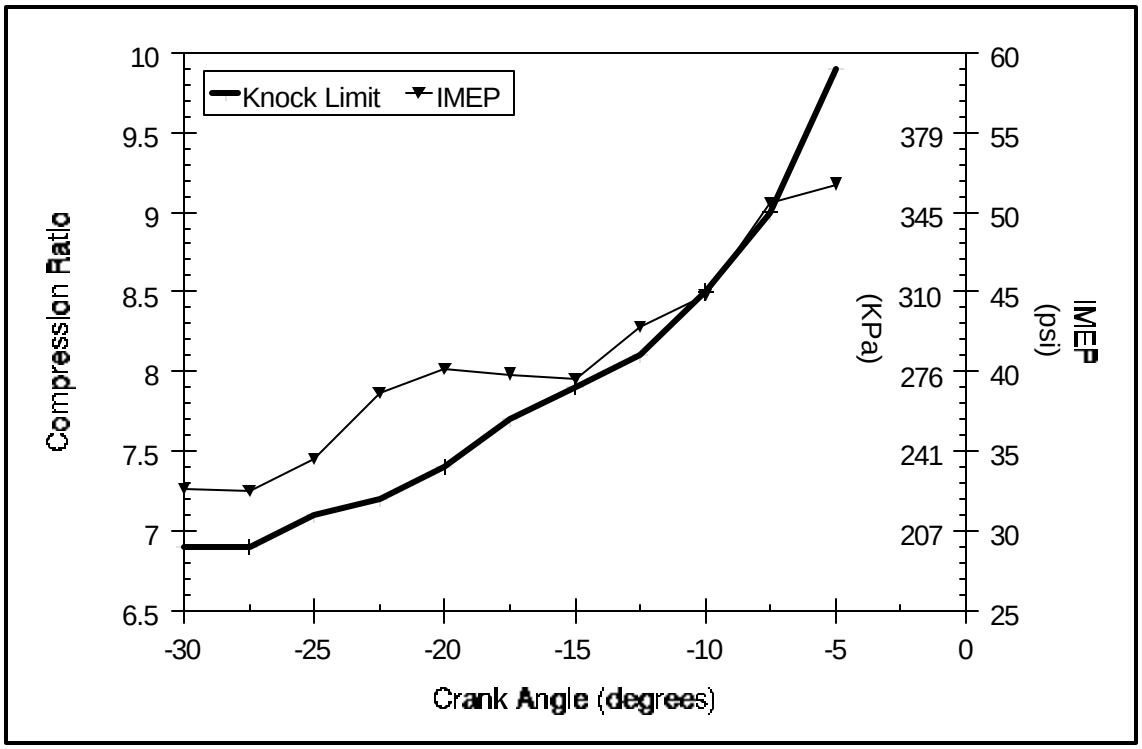

Figure 11 - Knock Limits and IMEP Trend for Blend 6

At the onset of blend testing, it was hoped that a KLCR could be found for the entire range of spark timings between 30^0 BTDC and 0^0. However, at spark timings above 5^0 BTDC, the KLCR could not be attained because the air/fuel mixture inside the cylinder would ignite, due to compression, before the occurrence of the spark (a phenomenon commonly called "dieseling") and the engine would not run properly. Thus, the KLCR/IMEP data only go up to 5^0 BTDC spark timing.

Knock Resistance Indicator and Antiknock Index

To determine the knock resistance capability of the blends over the range of spark timings, a Knock Resistance Indicator (KRI) was calculated from the KLCR vs. spark timing curves by numerically integrating the curves via the trapezoidal rule:

$$\mathrm{KRI} = \sum_{i=-27.5}^{-5\ (\text{by increment } 2.5)} \frac{1}{2}\left(\mathrm{KLCR}_i + \mathrm{KLCR}_{i\text{-}2.5}\right) \times 2.5 \qquad (8)$$

Where: KLCR_i = knock limiting compression ratio at spark timing *i*.

The KRI gives an indication of whether or not one blend allows higher compression ratios at the various spark timings than another blend, because it is the area under the KLCR vs. spark timing curve. The KRI for each blend is shown in Figure 12 along with the corresponding (RON+MON)/2 antiknock index. Figure 12 shows that both the KRI and the (RON+MON)/2 antiknock index increase with increasing oxygen content of the blend. The exceptions were blends 5 and 6, both of which contained 3.7% oxygen by mass. Blend 5 showed slightly better resistance to knock than blend 6. This indicates that lower alcohols enhance the anti-knock characteristics of the blends. Blend 5 contained 5.64% methanol/ethanol3 and 4.36% higher alcohols, whereas blend 6 contained 5.44% methanol/ethanol and 4.56% higher alcohols. The same conclusion can be drawn from blends 1 and 2. Blend 1, which contained 2.67% methanol/ethanol and 7.33% higher alcohols, showed greater anti-knock capability than blend 2, which contained 0.82% methanol/ethanol and 9.18% higher alcohols. Blends 3 and 4 further support the conclusion that the lower the order of the alcohol, the greater the anti-knock characteristics. Blends 3 and 4 contained identical quantities of methanol, ethanol, and propanol. However, blend 3, which contained 2.88% butanol and 0.13%, pentanol had better anti-knock characteristics than blend 4, which contained 0.12% butanol and 2.88% pentanol. In addition, blends 1 and 2 had the least resistance to knock than any of the others and contained the least amount of methanol/ethanol and the highest amount of higher alcohols. Blends 5 and 6 that exhibited the greatest resistance to knock than any others, contained the most methanol/ethanol and the least higher alcohols.

3 A percentage of methanol/ethanol indicates the percentage of methanol and ethanol combined. For example, 5% methanol/ethanol means that methanol and ethanol made up 5% of the total blend composition.

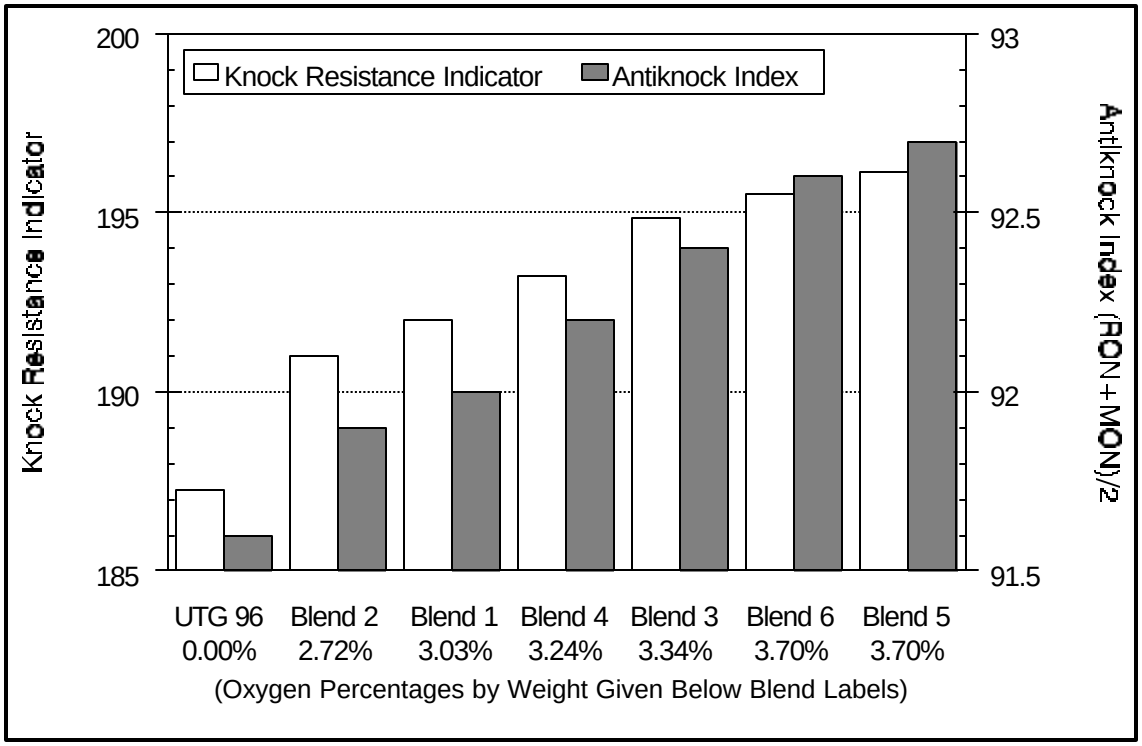

Figure 12 - Comparison of Knock Resistance Indicator and Antiknock Index Between Blends and UTG 96

Heat Release, MFB, Combustion Intervals, and Ignition Delays

The heat release and MFB curves are presented for each blend and UTG 96 in Figures 13 - 19. The ignition delays and combustion intervals are shown in Figure 20. It should be noted that the heat release data were taken at the spark timing/KLCR combination where the engine produced the maximum power for the blend in question (summarized in Table 6).

Heat release is the amount of heat that would have to be added to the cylinder contents to produce the measured pressure variations due to combustion of the air/fuel mixture. The heat release profiles shown for all the blends and UTG 96 in Figures 13 - 19 are very similar in shape and magnitude. The MFB curves were derived from the heat release data by numerically integrating the heat release curve up to the point of interest and dividing by the total heat released. The MFB curves shown in Figures 13 - 19 are also very similar in shape.

Ignition delay and combustion interval, defined earlier, give insight into the flame speed of a particular fuel. The shorter the ignition delay, the less time it takes for the flame to develop and vice versa. The shorter the combustion interval, the faster the flame burns the bulk of the charge and vice versa.

Figure 20 shows that both the ignition delay and combustion interval decrease with increasing oxygen content of the fuel. This indicates that increasing the oxygen content results in a decrease in flame development time and an increase in the burning velocity of the fuel. Blends 5 and 6, which had the same oxygen content, have identical ignition delays, but blend 6 showed a slightly shorter combustion interval. Hence, the greater the percentage of lower alcohols in the blends, higher is the flame speed. Blend 6 contained slightly more lower alcohols than blend 5. Similar trend was observed for blends 1 and 2. Blend 1, which contained 2.67%

methanol/ethanol and 7.33% higher alcohols, experienced a shorter ignition delay and combustion interval than blend 2, which contained 0.82% methanol/ethanol and 9.18% higher alcohols. Further, blends 3 and 4 illustrate an increase in flame speed a higher percentage of a lower order alcohol. Blends 3 and 4 contained identical amounts of methanol, ethanol, and propanol. However, blend 3, which contained 2.88% butanol and 0.13% pentanol, experienced a shorter combustion interval and ignition delay than blend 4, which contained 0.12% butanol and 2.88% pentanol.

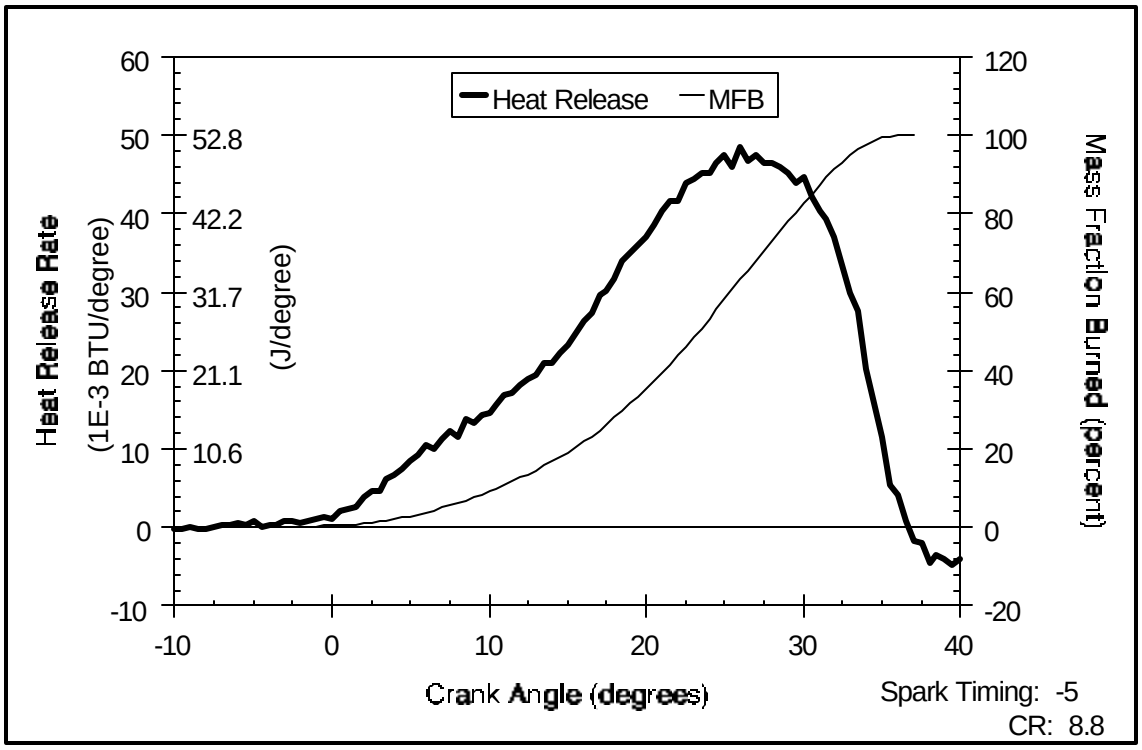

Figure 13 - Heat Release and MFB Curves for UTG 96

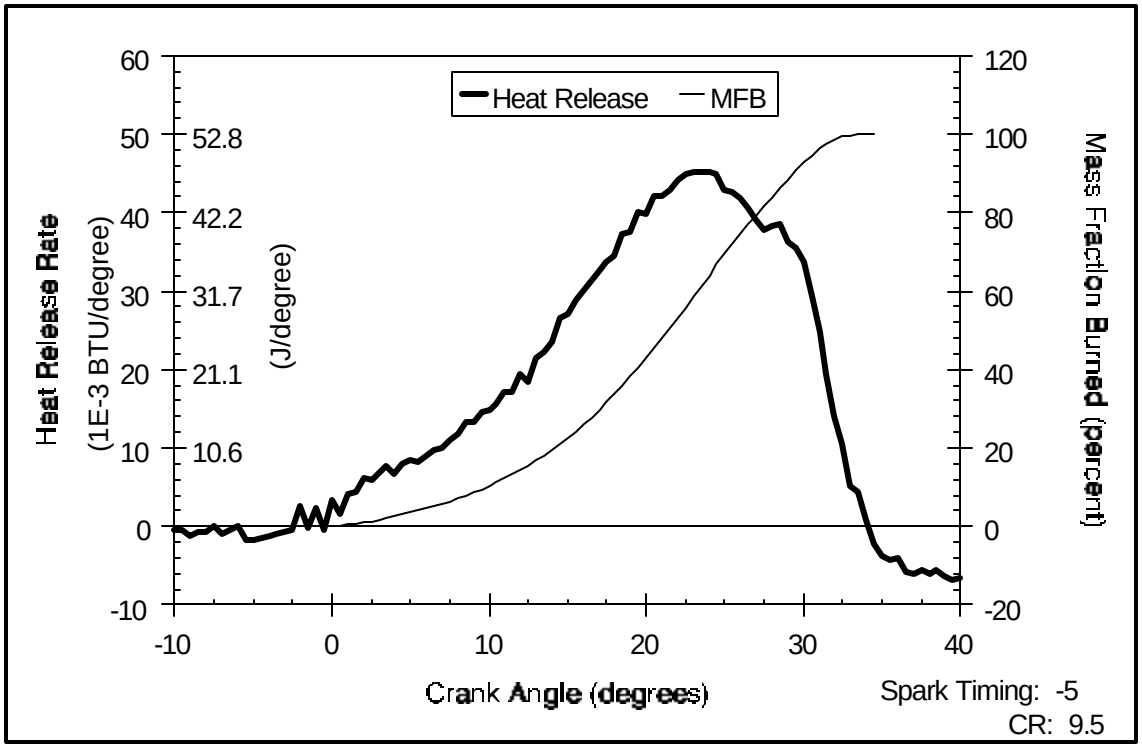

Figure 14 - Heat Release and MFB Curves for Blend 1

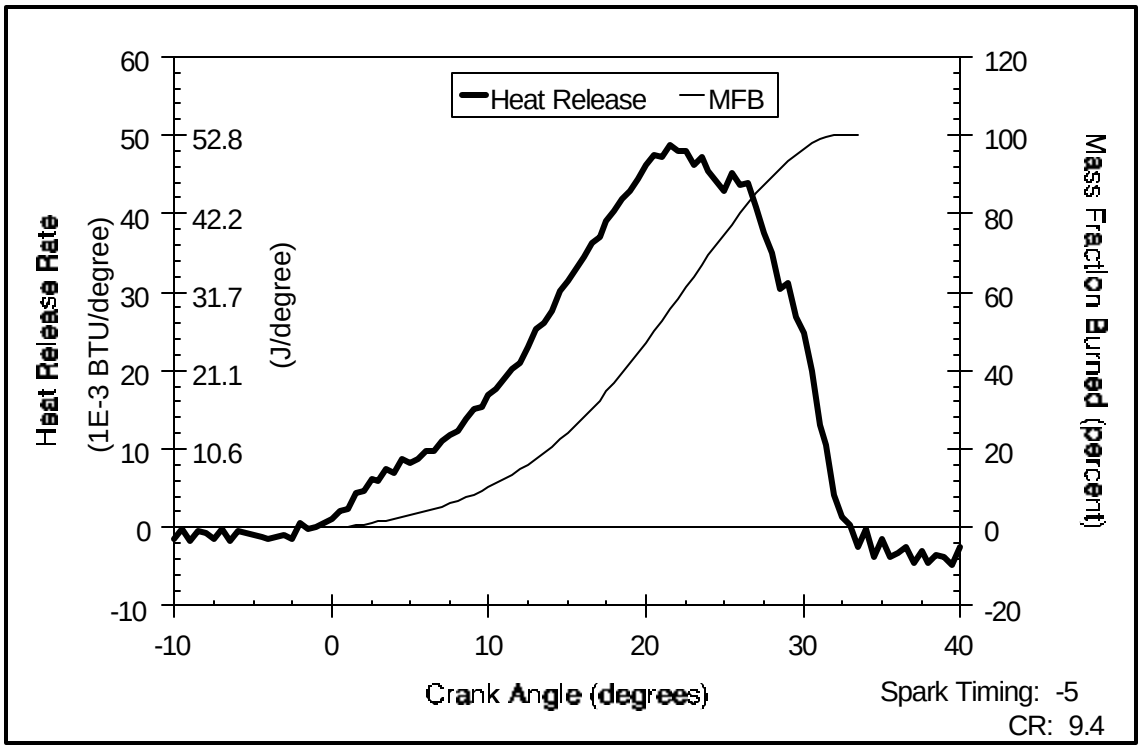

Figure 15 - Heat Release and MFB Curves for Blend 2

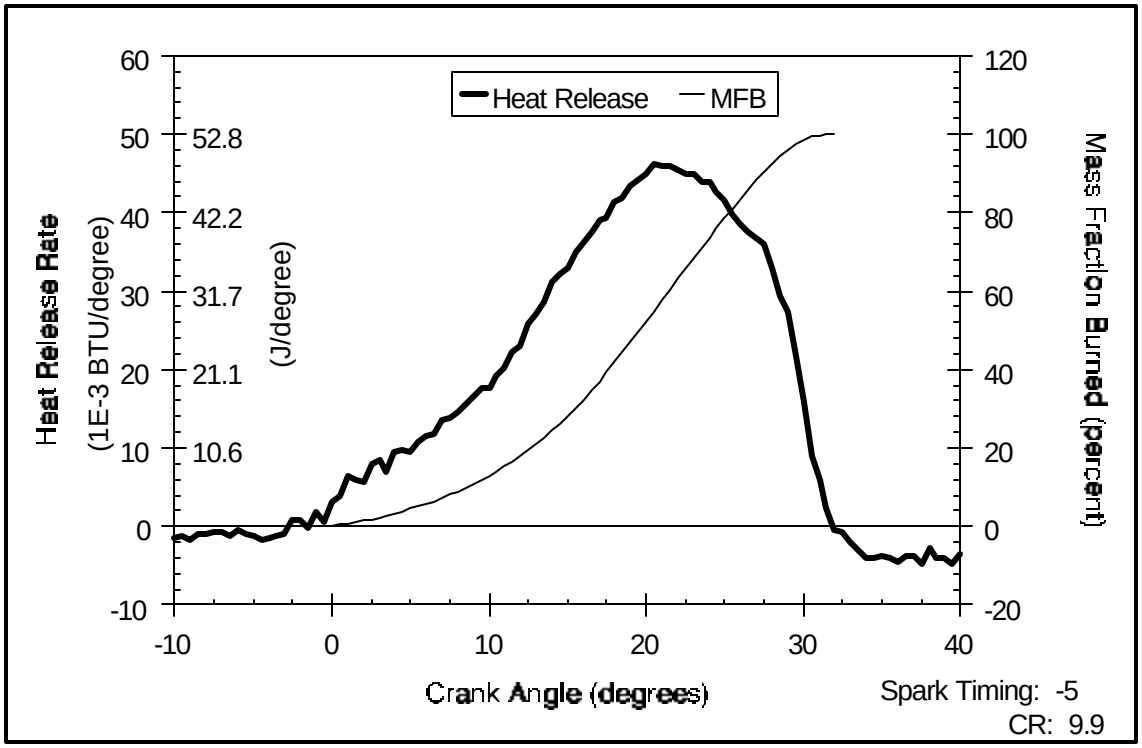

Figure 16 - Heat Release and MFB Curves for Blend 3

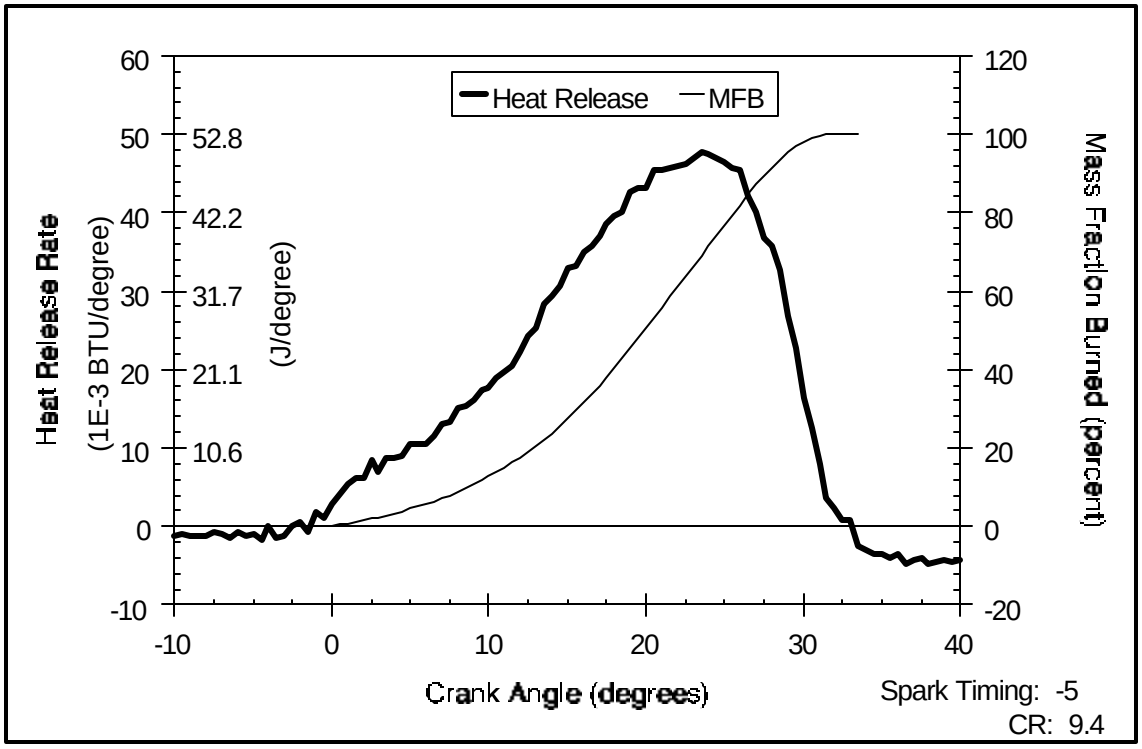

Figure 17 - Heat Release and MFB Curves for Blend 4

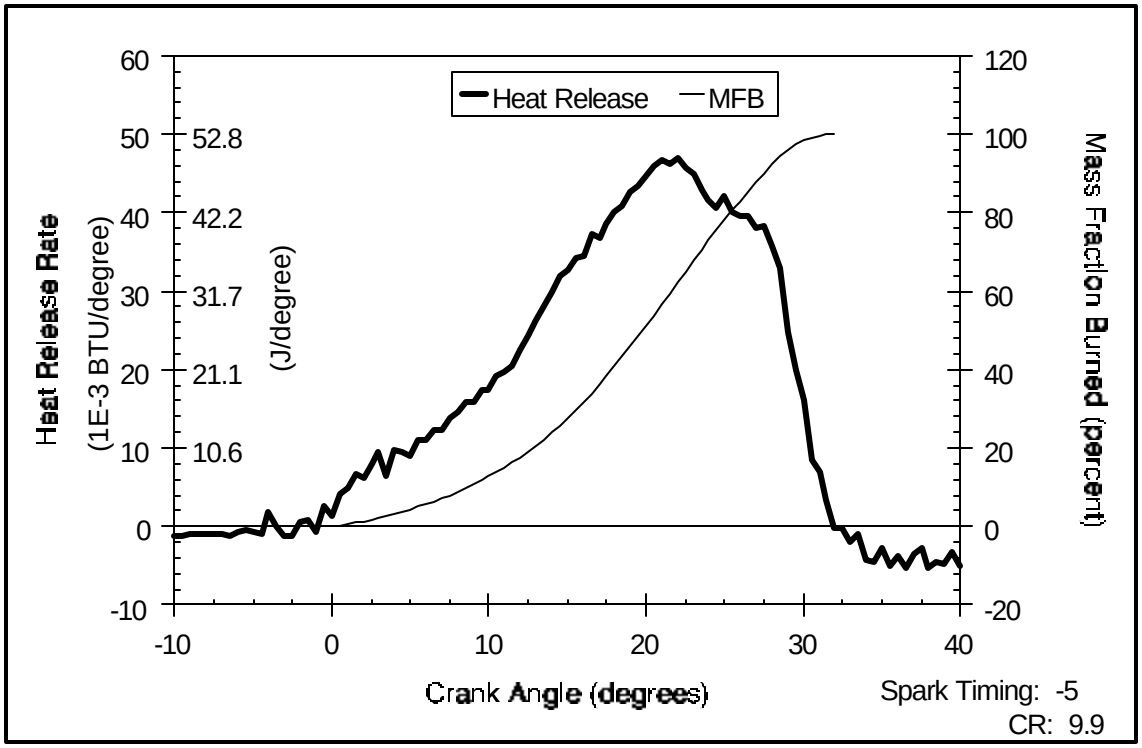

Figure 18 - Heat Release and MFB Curves for Blend 5

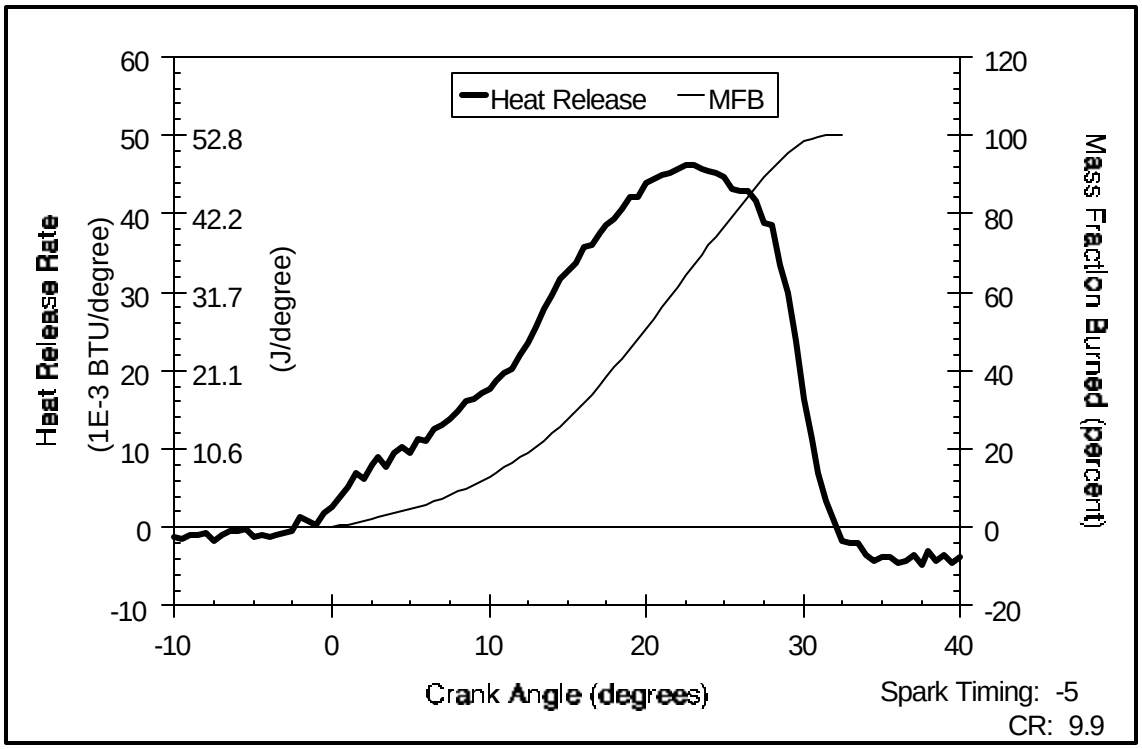

Figure 19 - Heat Release and MFB Curves for Blend 6

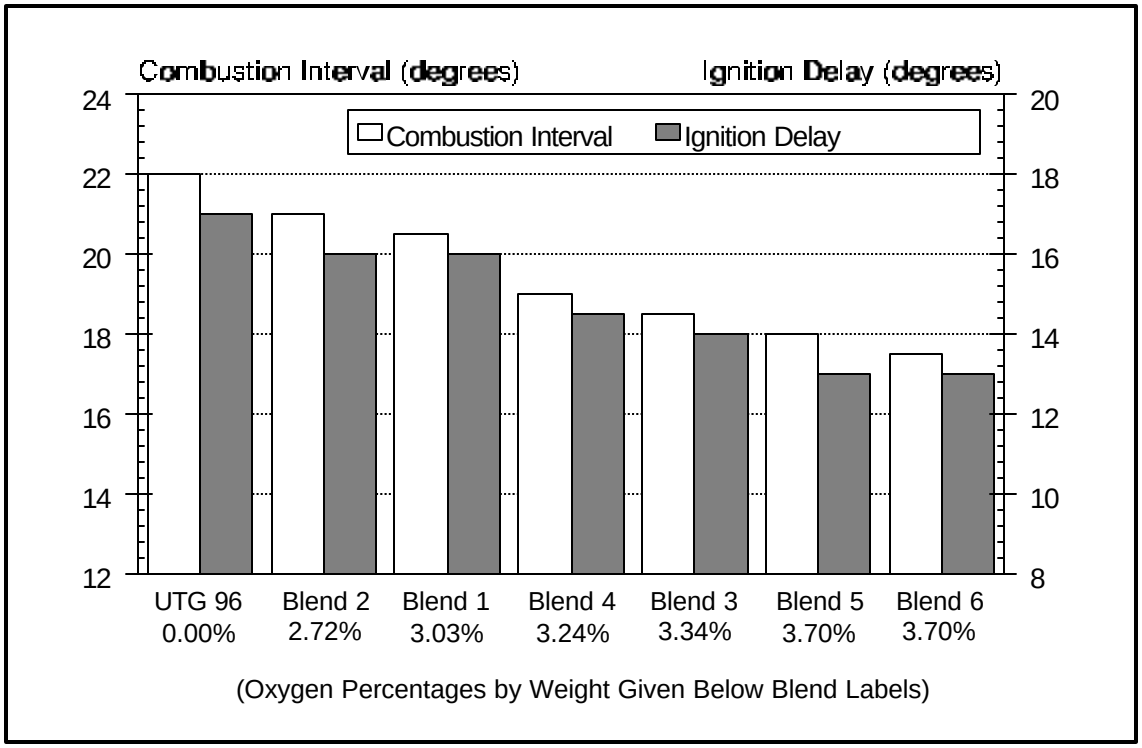

Figure 20 - Comparison of Ignition Delays and Combustion Intervals Between Blends and UTG 96

Reid Vapor Pressure and Distillation

The RVP for each blend and UTG 96 is shown in Figure 21. The higher the RVP, the more difficult it is to control evaporative emissions. Blend 1 (2.67% methanol/ethanol, 7.33% higher alcohols) showed only a slight increase in RVP compared to UTG 96, and blend 2 (0.82% methanol/ethanol, 9.18% higher alcohols) actually showed a small decrease in RVP compared to UTG 96. Blends 5 and 6 had the highest RVP out of all the blends, and these two blends also contained the highest amounts of the lower alcohols (5.64% methanol/ethanol for blend 5 and 5.44% methanol/ethanol for blend 6). Blends 3 and 4 also showed how higher order alcohols help control the RVP of the blend, because blend 4 had an RVP lower than blend 3. Blends 3 and 4 were identical except that blend 3 contained 2.88% butanol and 0.12% pentanol, whereas blend 4 contained 0.12% butanol and 2.88% pentanol. Another aspect of blends 5 and 6 illustrates how high order alcohols can offset the effects on RVP from lower alcohols. Blend 5 contains 3.24% methanol compared to 3.04% methanol in blend 6. However, these two blends have nearly identical RVPs. The fact that blend 5 contains 1.47% pentanol compared to 0.13% pentanol in blend 6 seems to offset the higher concentration of methanol in blend 5.

It has been shown by previous researchers that the presence of alcohols in gasoline depresses the distillation curve of the fuel, which can cause problems with cold starting and vapor lock. This expected trend was true of the six test blends. The distillation curves for each of the blends, are compared to UTG 96 in Figures 23-28. The distillation curve for each blend was significantly depressed between 0% and 60% . To determine the effects of the different alcohols on the distillation curve, the area under each curve between 0% and 60% evaporated was numerically calculated (see Figure 29). The distillation curves for blends 1 and 2 were the

least affected by the alcohols. It should be noted that these blends also contain the least methanol/ethanol. The distillation curve for blend 2 was less affected than blend 1, and, as mentioned previously, blend 2 had lower methanol/ethanol concentration than blend 1. Blends 5 and 6 showed the most pronounced effect on the distillation curve, and these blends contain the most methanol/ethanol. Thus, it becomes obvious that the lower alcohols have a more significant effect on the distillation curve than the higher alcohols.

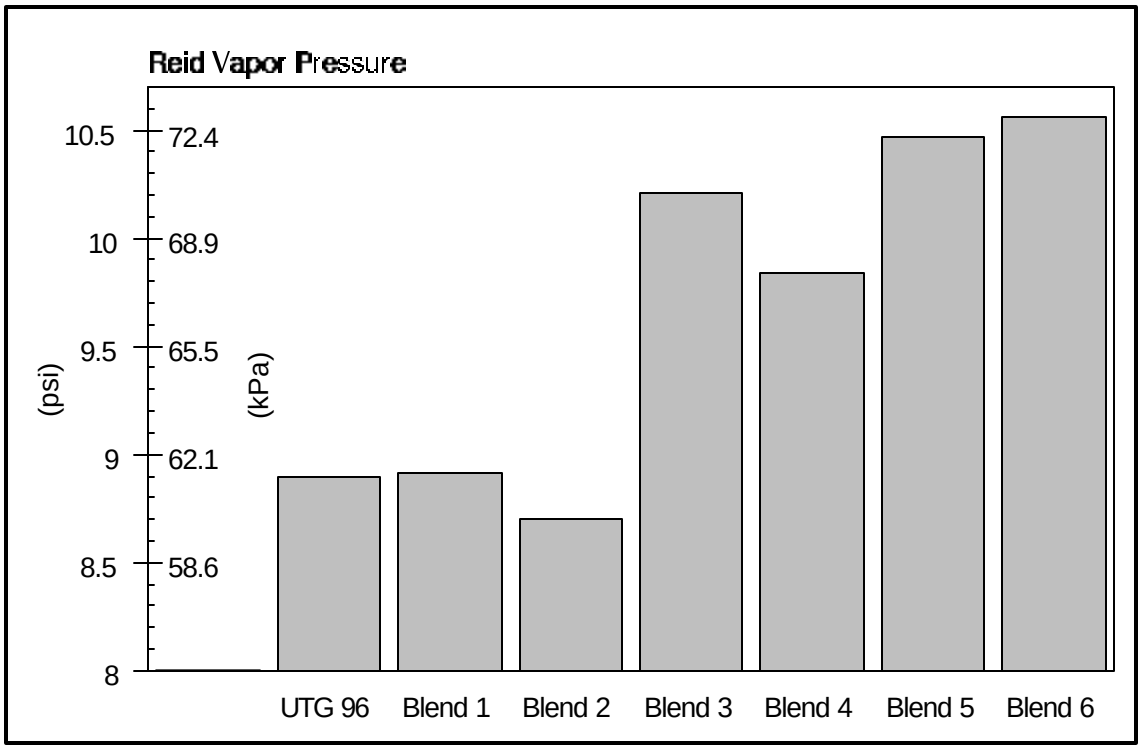

Figure 21 - Reid Vapor Pressures of the Blends and UTG 96

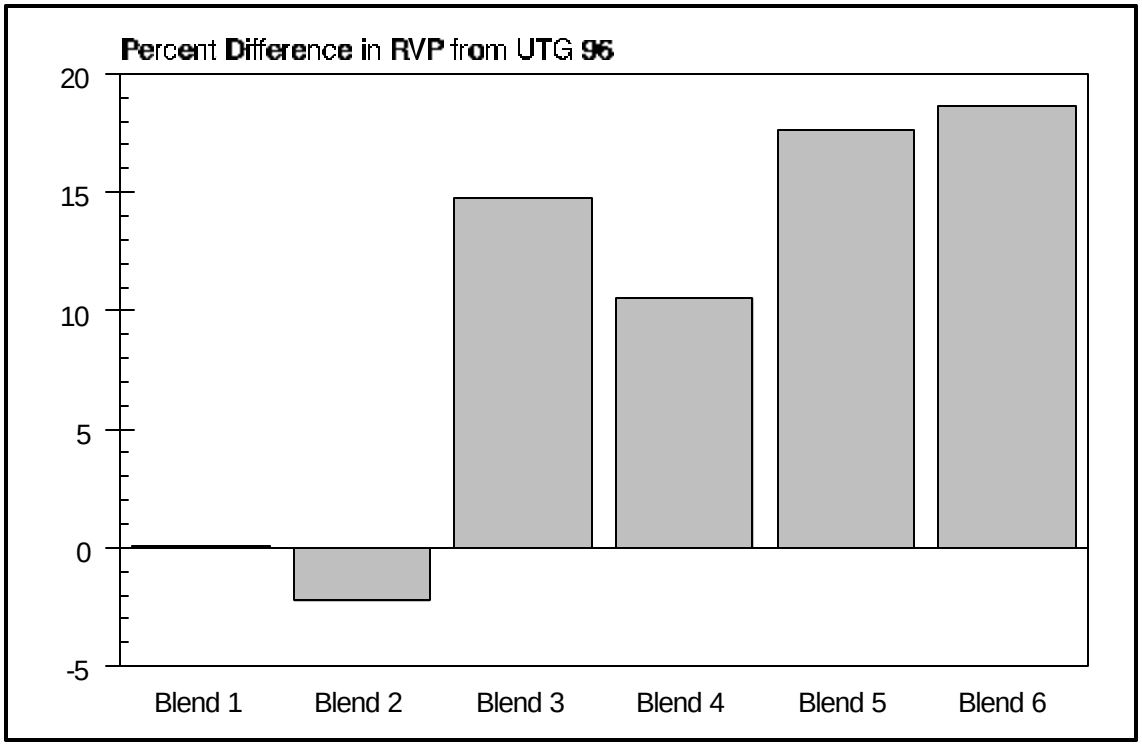

Figure 22 - Percent Difference in RVP Between Blends and UTG 96

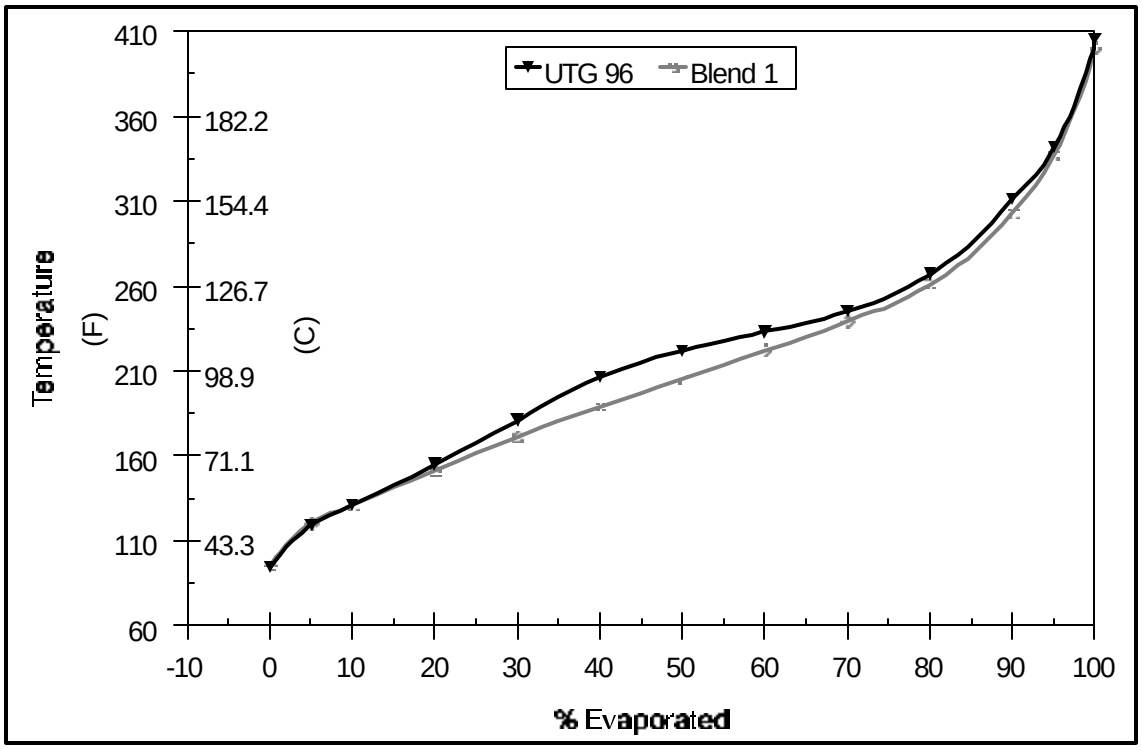

Figure 23 - Comparison of Distillation Curves Between Blend 1 and UTG 96

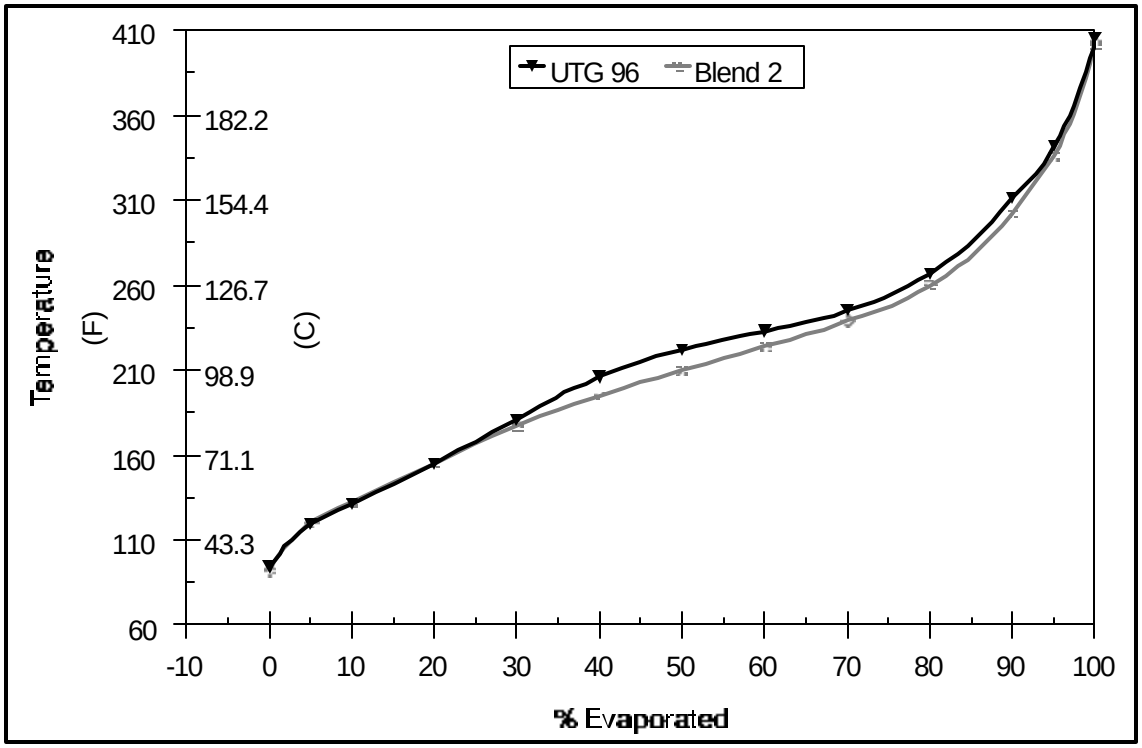

Figure 24 - Comparison of Distillation Curves Between Blend 2 and UTG 96

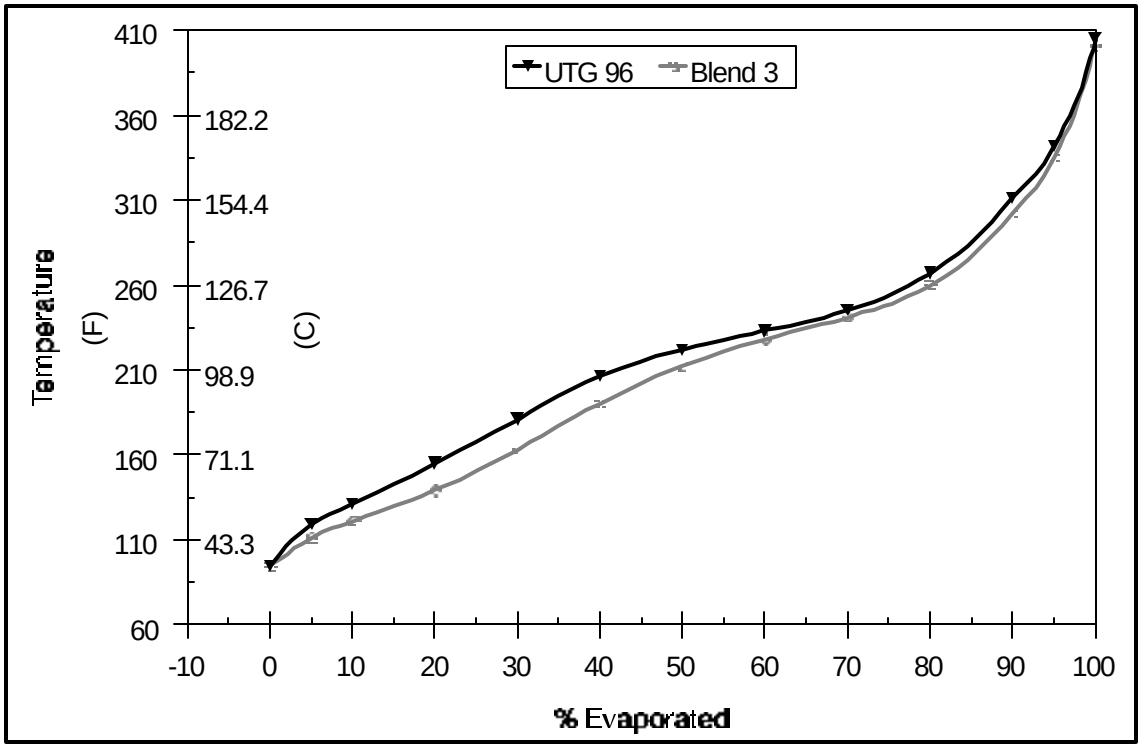

Figure 25 - Comparison of Distillation Curves Between Blend 3 and UTG 96

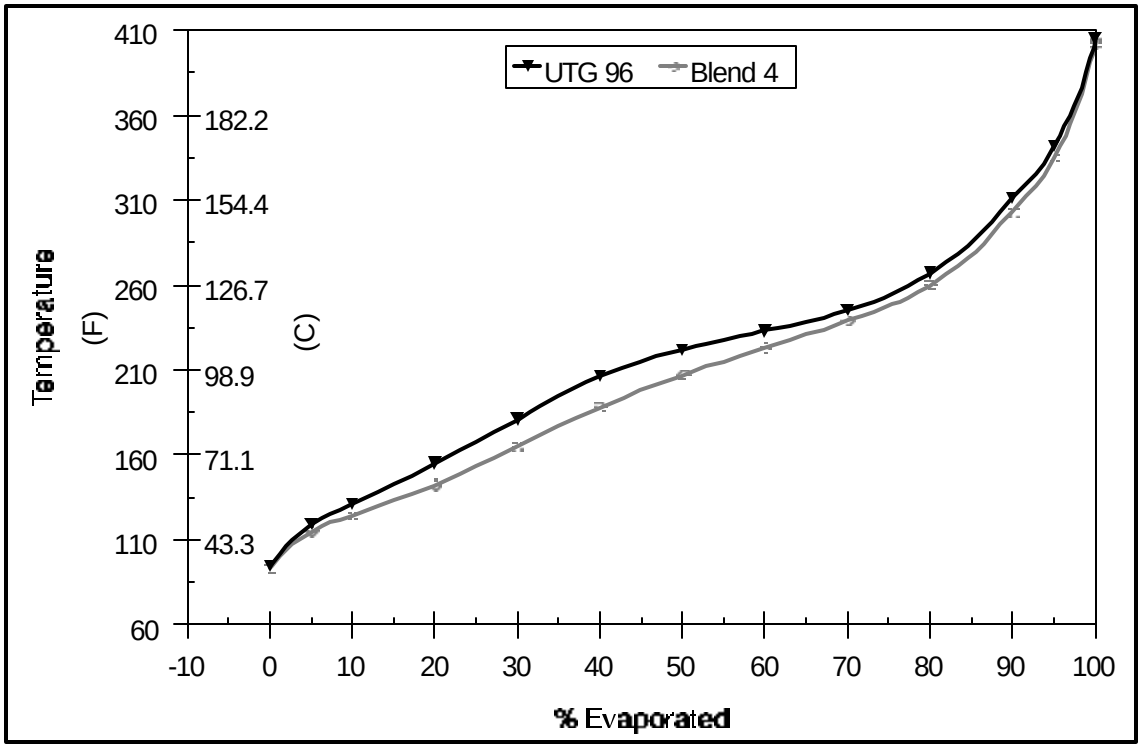

Figure 26 - Comparison of Distillation Curves Between Blend 4 and UTG 96

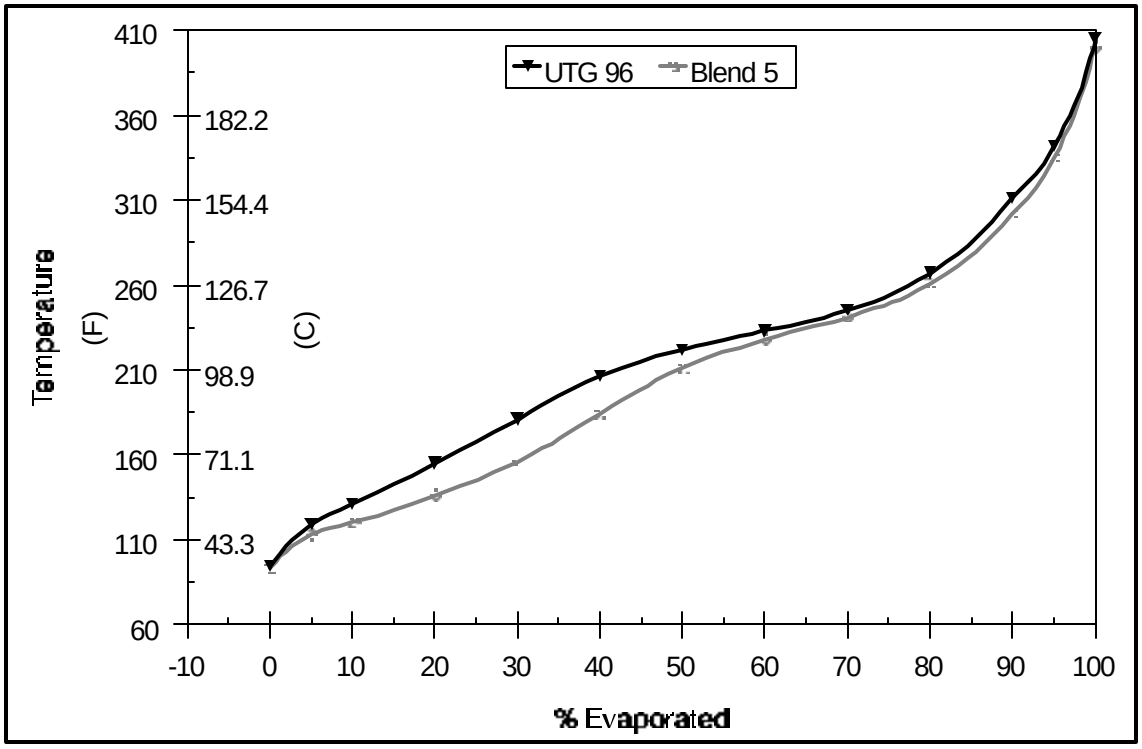

Figure 27 - Comparison of Distillation Curves Between Blend 5 and UTG 96

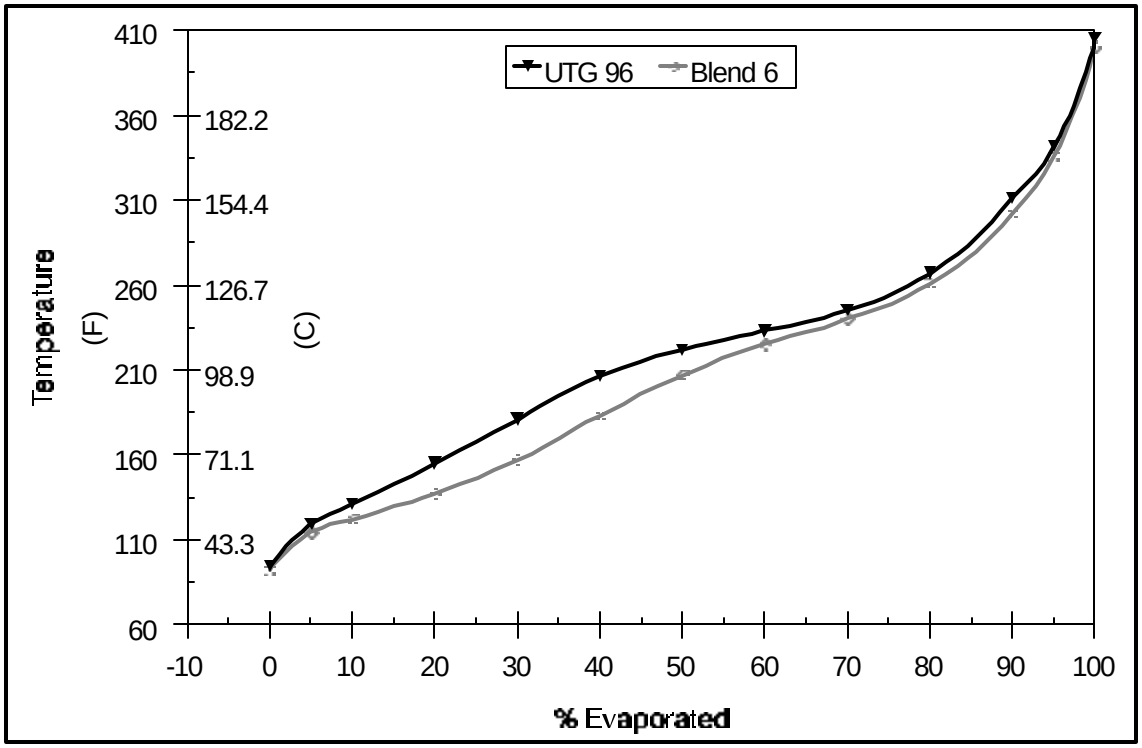

Figure 28 - Comparison of Distillation Curves Between Blend 6 and UTG 96

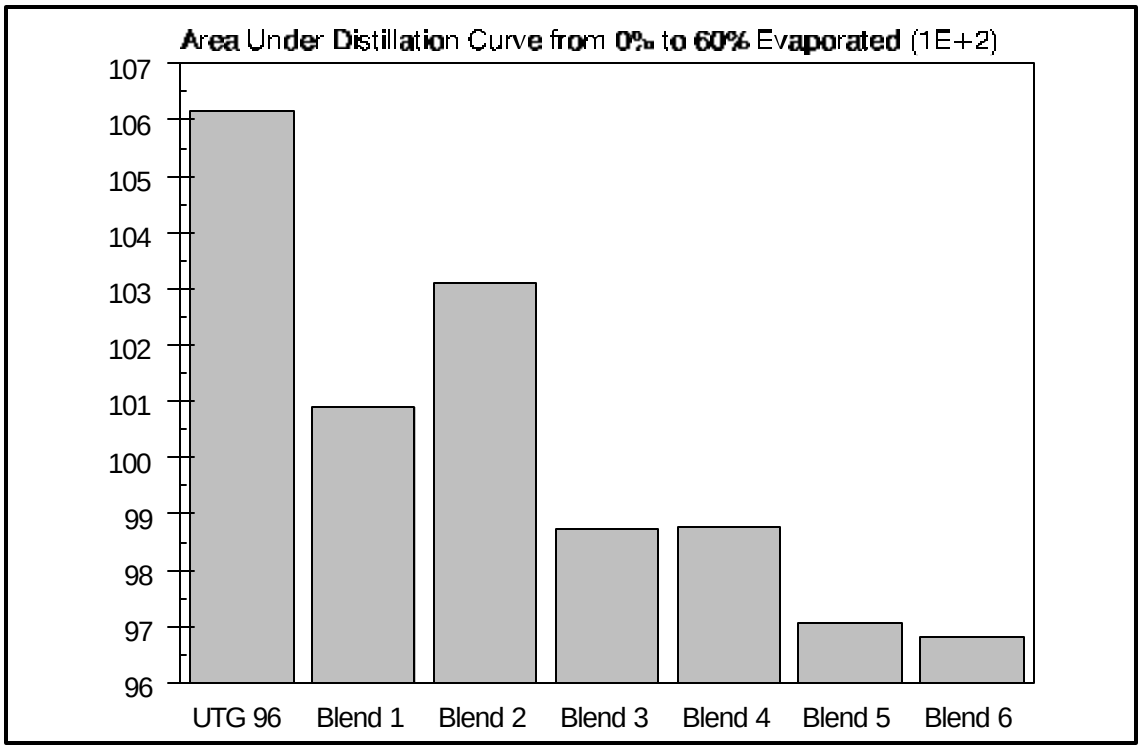

Figure 29 - Comparison of the Area Under the Distillation Curve Between 0% and 60% Evaporated for the Blends and UTG 96

Conclusions

An experimental investigation of combustion characteristics of higher alcohols/gasoline (UTG 96) blends was conducted. A single-cylinder ASTM-CFR engine was instrumented and the necessary data acquisition and corresponding data reduction computer programs were developed and implemented. Comparisons of knock limits, best IMEP, and fuel characteristics between higher alcohol/gasoline blends and neat gasoline were made to determine the advantages and disadvantages of blending higher alcohols with gasoline. All tests were conducted on the single-cylinder Waukesha CFR engine at steady state conditions and stoichiometric air-to-fuel ratio. The knock limiting compression ratio (KLCR) was found at spark timings ranging from 30^0 before top dead center (BTDC) and 5^0 BTDC by increments of 2.5^0, and the corresponding indicated mean effective pressures (IMEPs) at these points were recorded. The data show that for each fuel blend tested, the best IMEP occurred at a spark timing of 5^0 BTDC and the corresponding KLCR. In addition, the higher alcohol/gasoline blends show a much better resistance to knock than neat gasoline, as indicated by the knock resistance indicator (KRI) and the (RON+MON)/2 antiknock index. The overall ability of the blends to resist knock seems to be a function of the total oxygen content of the blend; the higher the oxygen content there is in the blend, the higher the knock resistance. Ignition delay and combustion interval data show that higher alcohol/gasoline blends tend to have faster flame speeds. Here again, the oxygen content plays a role since the higher oxygen content blends tended to have faster flame speeds than the lower oxygen content blends.

The other fuel parameters, RVP and distillation curve, are affected by the addition of alcohol to gasoline. The lower alcohols (methanol and ethanol) cause the most dramatic increase in RVP and the largest depression of the distillation curve. Addition of the higher alcohols (propanol, butanol, and pentanol) seemed to curb the effects of methanol and ethanol on RVP and distillation.

References

Bardon, M.F., Gardiner, D.P., and Rao, V.K., "Cold Starting Performance of Gasoline/Methanol M10 Blends in a Spark Ignition Engine", SAE Paper No. 85204, 1985

Bata, R. M., Elrod, Alvon C., and Lewandowski, T. P., "Butanol as a Blending Agent with Gasoline for I.C. Engines," SAE Paper No. 890434, 1989.

Brinkman, N. D., Galloupoulous, N. E., and Jackson, M. W., "Exhaust Emissions, Fuel Economy, and Driveability of Vehicles Fueled with Alcohol-Gasoline Blends," SAE Paper No. 750120, 1975.

Chapra, Steven C., and Canale, Raymond P., Numerical Methods for Engineers, Second Edition, McGraw-Hill, Inc., 1988.

Checkel, M. D., and Dale, J. D., "Computerized Knock Detection from Engine Pressure Records," SAE Paper No. 860028, 1986.

Coordinating Research Council, Inc., "1982 CRC Fuel Rating Program: Road Octane Performance of Oxygenates in 1982 Model Cars," CRC Report Number 541, July 1985.

Dean, John A., Lange's Handbook of Chemistry, 14th Edition, McGraw-Hill, Inc., New York, NY, 1992.

Dorn, P., Maurao, A. M., and Herbstman, S., "The Properties and Performance of Modern Automotive Fuels," SAE Paper No. 861178, 1986.

Ebersole, G. D., and Manning, F. S., "Engine Performance and Exhaust Emissions: Methanol versus Isooctane," SAE Paper No. 720692, 1972.

Harrington, J. A., and Pilot, R. M., "Combustion and Emission Characteristics of Methanol," SAE Paper No. 750420, 1975.

Heywood, John B., Internal Combustion Engine Fundamentals, McGraw-Hill, Inc., 1988.

Hunwartzen, I., "Modification of CFR Test Engine Unit to Determine Octane Numbers of Pure Alcohols and Gasoline-Alcohol Blends," SAE Paper No. 820002, 1982.

Martin II, Daniel W., "Combustion and Emissions Characteristics of Higher Alcohol/Gasoline Blends," Masters Thesis, West Virginia University, Department of Mechanical and Aerospace Engineering, 1997.

Oppenheim, A. K., "The Knock Syndrome - Its Cures and Its Victims," SAE Paper No. 841339, 1984.

Patel, K. S., and Henein, N. A., "Burning Velocities in Methanol-Indolene Air Mixtures in a CFR Engine," SAE Paper No. 850111, 1985.

Patel, K. S., Kumar, S., and Kwon, O. Y., "The Performance Characteristics of Indolene-MPHA Blends in a Spark Ignition Engine," SAE Paper No. 872068, 1987.

Phillips 66, Certificate of Analysis of Unleaded Test Gas 96, Lot No. W-061A, Shipped 10/23/1995.

Stone, Richard, Introduction to Internal Combustion Engines, Society of Automotive Engineers, Warrendale, PA, 1994.

Unzelman, G. H., "Octane Improvement in the 1990's," NPRA Paper AM-88-25, National Petroleum refiners Association Annual Meeting, March 1988.

Yaccarino, P. A., "Hot Weather Driveability and Vapor-Lock Performance With Alcohol-Gasoline Blends," SAE Special Publication SP-638, 1985.